ISSN 0001-4370, Oceanology, 2013, Vol. 53, No. 5, pp. 570–606. © Pleiades Publishing, Inc., 2013.
Original Russian Text © A.Yu. Lein, P.N. Makkaveev, A.S. Savvichev, M.D. Kravchishina, N.A. Belyaev, O.M. Dara, M.S. Ponyaev, E.E. Zakharova, A.G. Rozanov, M.V. Ivanov, M.V. Flint, 2013, published in Okeanologiya, 2013, Vol. 53, No. 5, pp. 643–679.

MARINE GEOLOGY

Transformation of Suspended Particulate Matter into Sediment in the Kara Sea in September of 2011

A. Yu. Lein[a], P. N. Makkaveev[a], A. S. Savvichev[b], M. D. Kravchishina[a], N. A. Belyaev[a], O. M. Dara[a], M. S. Ponyaev[a], E. E. Zakharova[b], A. G. Rozanov[a], M. V. Ivanov[b], and M. V. Flint[a]

[a] *Shirshov Institute of Oceanology, Russian Academy of Sciences, Russia*
e-mail: lein@ocean.ru
[b] *Winogradskii Institute of Microbiology, Russian Academy of Sciences, Russia*
e-mail: savvichev@mail.ru

Received November 28, 2012; in final form, January 12, 2013

Abstract—The biogeochemical processes participating in the transformation of the particulate matter into sediment along the Yenisei River–St. Anna Trough (Kara Sea) meridional profile were studied using hydrochemical, geochemical, microbiological, radioisotope, and isotope methods. The water–sediment contact zone consists of three subzones: the suprabottom water, the fluffy layer, and the surface sediment. The total number, biomass, and integral activity of the microorganisms (dark $^{14}CO_2$ assimilation) in the fluffy layer are usually higher than in the suprabottom water and sediment. The fluffy layer shows a decrease in the oxygen content and the growth of the dissolved biogenic elements. It was provided by the particulate organic matter supporting the vital activity of the heterotrophs from the overlying water column and by the flux of reduced compounds (NH_4, H_2S, CH_4, Fe^{2+}, Mn^{2+}, and others) from the underlying sediments. The C_{org} isotopic composition of the fluffy layer and the sediments is 2–4 ‰ heavier than that of the particulate matter and sediment due to the presence of the isotopically heavy biomass of microorganisms. A change in the isotopic composition of the C_{org} in the fluffy layer and surface sediment as compared to the C_{org} of the particulate matter is a widespread phenomenon in the Arctic shelf seas and proves the leading role of microorganisms in the transformation of the particulate matter into sediment.

DOI: 10.1134/S0001437013050081

INTRODUCTION

The transformation of the particulate matter of the water sequence into sediment is governed by different processes, including the biogeochemical cycles, which operate over the entire pathway of the particulates from the drainage area to the sea, being most the intense at the water–bottom boundary.

Quantitative studies of the rate of the biogeochemical processes and the number of microorganisms participating in them using radioisotope tracers were launched in the water column and sediments of the Kara Sea in 1993 [15, 16, 19, 20] and continued in 2007 [26]. In August–September of 2001, the total number of bacteria and the value of the bacterial production were studied in the Kara Sea using the method of tritiated leucine [33].

For the last ten years, the experimental data on the distribution and composition of the organic carbon [the dissolved organic carbon (DOC) and the particulate organic carbon (POC)] in the water column and sediments of the Kara Sea were obtained and generalized [5, 24, 31, 38, 39]. For objective reasons (primarily, due to the absence of a sampling device), the biogeochemical processes proceedings at the water column–sediment boundary were the least studied. The first data were reported in [9, 13, 14].

The appearance of such samplers as the Niemiste pipe and multicorer samplers, which allow the preservation of the water–sediment contact zone, offers the possibility for the detailed study of this zone, one of two major barrier zones in seas and oceans, together with the water–atmosphere contact zone.

The aim of this work was to study the biogeochemical transformations of the particulate matter into the sediment using hydrochemical, chemical, microbiological, isotope, and radioisotope methods.

MATERIALS AND METHODS

The samples were collected using Niskin bottles mounted on a Rosette sampler (the water collected) and a multicorer (the suprabottom water, the fluffy layer, and the sediment). In total, we studied 20 sites along a submeridional profile from the Yenisei River's mouth to the St. Anna Trough (Fig. 1).

The sampling and the study of the particulate matter comprises simultaneous vacuum filtration via nuclear membrane and fiberglass (GF/F) filters and

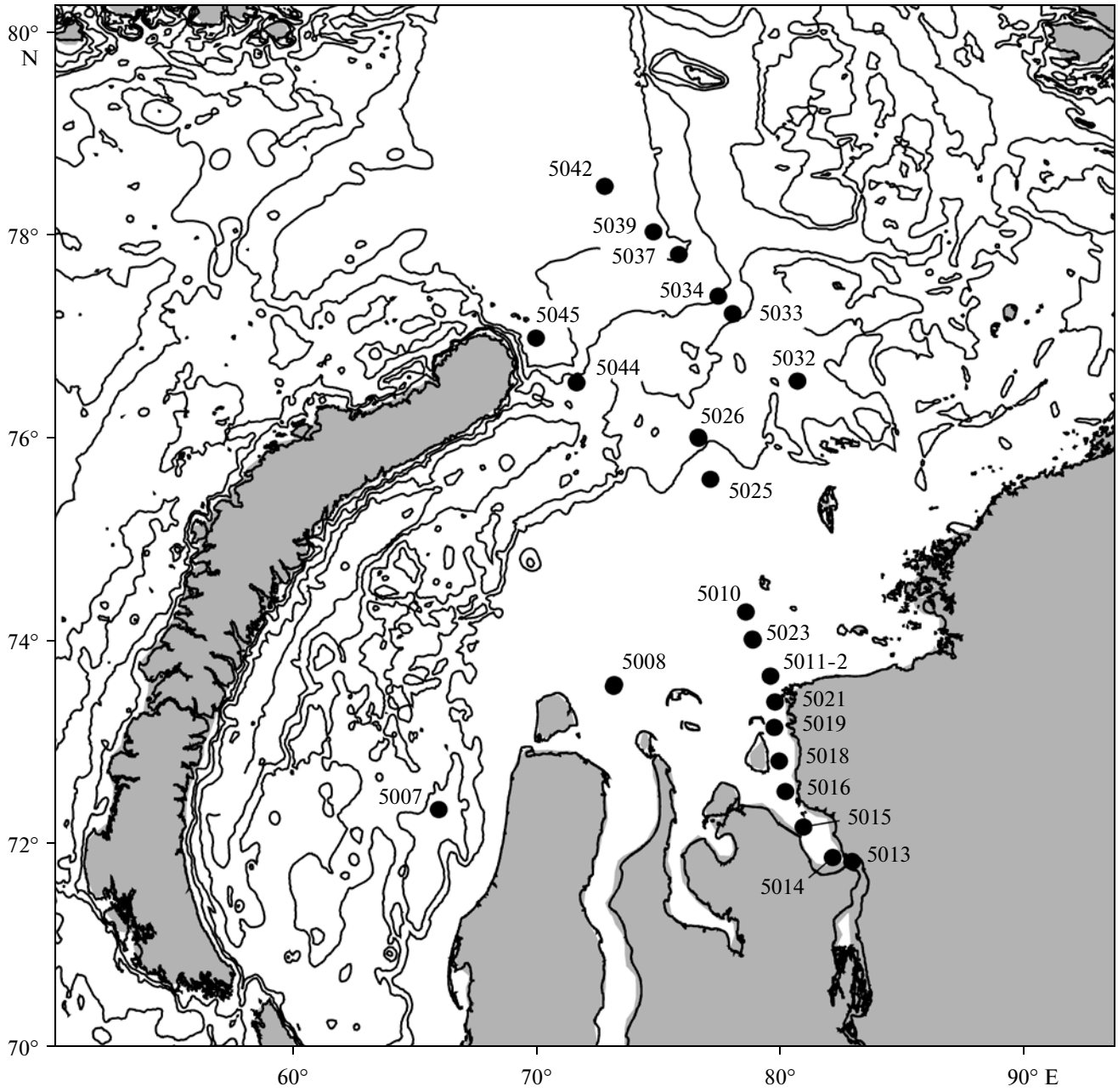

Fig. 1. Schematic location of the sites of the water and sediment sampling during Cruise 59 of the R/V *Akademik Mstislav Keldysh* in the Kara Sea.

the analysis of the grain-size composition of the particulate matter using a Coulter counter [11].

Nuclear membrane filters were used to determine the concentration of particulate matter and to study its mineral and element chemical composition.

The materials from the fiberglass filters were analyzed to obtain the content and isotope composition ($\delta^{13}C$) of the organic (C_{org}) and carbonate (C_{carb}) carbon.

Water samples were collected from the surface and near-bottom horizons (two meters from the bottom) of the water column by the Niskin bottles mounted on a Rosette sampler after the preliminary sounding. The samples were analyzed for their hydrochemical composition using the technique in [18], the carbon isotope composition of the bicarbonate ions [14], the contents of the dissolved organic carbon [1] and methane, and the total number of microorganisms (TNM). The integral rate of the microbial processes of the dark CO_2 assimilation (DCH) was determined by the methods described in [26].

Samples of the suprabottom water and the fluffy layer were taken from the multicorer using a pippete or

small injector. To analyze the suprabottom layer, the water was collected using a siphon from the multicorer pipes (from a water column 10–40 cm long). The wet sediment was taken from the cores and analyzed according to the layers. The sediments were pushed using a plastic piston from the vertical multicorer pipe by centimeters with the correction of the interlayer thickness using the lithological description. The chemical and mineral compositions of the sediments and the fluffy layer were determined, respectively, using the XRF and XRD methods. The content of C_{org} was analyzed using an AN-7560 express analyzer by recording the CO_2 during the annealing of the samples (T = 900°C) in CO_2-free air (the analyst was L.V. Demina) and using a TOC analyzer (the analysts were N.A. Belyaev and M.S. Ponyaev). The content of the normal hydrocarbons was determined by gas chromatography using a Shimadzu GC 2014 chromatograph. The isotopic composition of the carbonate and organic carbon was analyzed using a Delta Plus mass spectrometer (Germany). The measurement accuracy was ±0.1‰ [13].

The pore water was squeezed out onboard by centrifuging. The values of the pH, Eh, Alk, $P-PO_4$, Si, and N_{tot} were also analyzed onboard [18]. The salt composition of the pore waters (the SO_4, Cl, Ca, and Mg) was determined using the conventional chemical methods (the analyst was G.A. Pavlova) [27].

The rates of the biogeochemical processes in the sediments (the CO_2 assimilation, the sulfate reduction, and the methane genesis) were determined by the radioisotope method described in [6, 26]. The CH_4 content was measured by phase-equilibrium degassing using a gas chromatograph with a Cristal-200-OM flame-ionization detector. The content of the sulfur species was determined by systematic phase analysis (the analyst was N.M. Kokryatskaya) [4]. The total number of microorganisms was measured using the technique in [14].

RESULTS AND DISCUSSION

1. The hydrochemical Structure of the Waters along the Yenisei River–Kara Sea Profile

The Yenisei River–St. Anna Trough submeridional profile (further termed the meridional profile) was run in September 18–22, 2011, and spanned depths from 13 m (site 5014) to 476 m (site 5026) (Fig. 1). By the distribution of the water masses, the profile from the south northward is subdivided into the following zones: the fresh (river) waters → the mixing zone of the river and sea waters in the estuary → the inner shelf → the outer shelf → the open sea → the St. Anna Trough.

The salinity of the surface waters along the profile varies from 0.06 PSU (Table 1) to 33.4 PSU. At the southernmost site (no. 5013), saline seawaters are practically absent.

The modern hydrology of the Kara Sea is influenced by the Ob and Yenisei rivers' runoff. Note also that the suprabottom water has higher salinity: from 10–15 PSU in the estuary to 34.5 PSU on the outer shelf.

The river–sea water mixing zone during the cruise was characterized by a composite structure and consisted of a vertical frontal zone passing between sites 5013 and 5018 and a horizontal frontal zone spanning the southern part of the sea (up to site 5026), which is exemplified by the distribution of the total alkalinity (Alk).

The concentration of the dissolved oxygen along the profile varies from 5.5 mL L^{-1} in the near-bottom horizons of sites 5010 and 5023 to 9.0 mL L^{-1} at site 5026; i.e., the biological activity of the waters was insignificant even at the shoals and did not result in hypoxia. Higher contents of ammonium nitrogen as compared to the estuary and marine sites were determined in the water column of the three southern mouth sites.

The concentration of dissolved organic carbon in the surface layer of the water column varies from 5.95 mg L^{-1} in the mouth (site 5013) to 3.24 mg L^{-1} on the shelf (site 5026) (Table 1, Fig. 2). The dissolved organic carbon produced conservative variations, which are closely related to the desalination of the Kara Sea waters by the DOC-rich Yenisei runoff.

The concentration of the particulate organic carbon in the surface layer decreases from 407 μg L^{-1} at mouth site 5014 to 66 μg L^{-1} at shelf site 5042 (Fig. 2b). In contrast, the fraction of organic carbon in the suspended matter increases from the mouth to the shelf (Table 1), which may be related both to the elevated precipitation of the suspended mineral component at the river–sea barrier and the enrichment of the suspended matter in the newly formed autochthonous organic matter.

The concentration of the particulate matter in the surface layer of the water column decreases from 2.55 mg L^{-1} at the mouth (site 5013) to 0.34 mg L^{-1} at the shelf (site 5026), i.e., by almost nine times (Table 1, Fig. 3). Thus, we observe an opposite correlation between the salinity and the concentration: the higher the salinity, the lower the concentration of the particulate matter.

Downward the water column, the concentration of the particulate matter usually increases at the sites subjected to the strong influence of the river waters and remains practically unchanged at the seaward sites. Its maximal contents were found in the near-bottom layers of the water column at sites 5015 and 5021 (Fig. 3).

The isotopic composition of the particulate organic carbon is also related to the concentration of the sus-

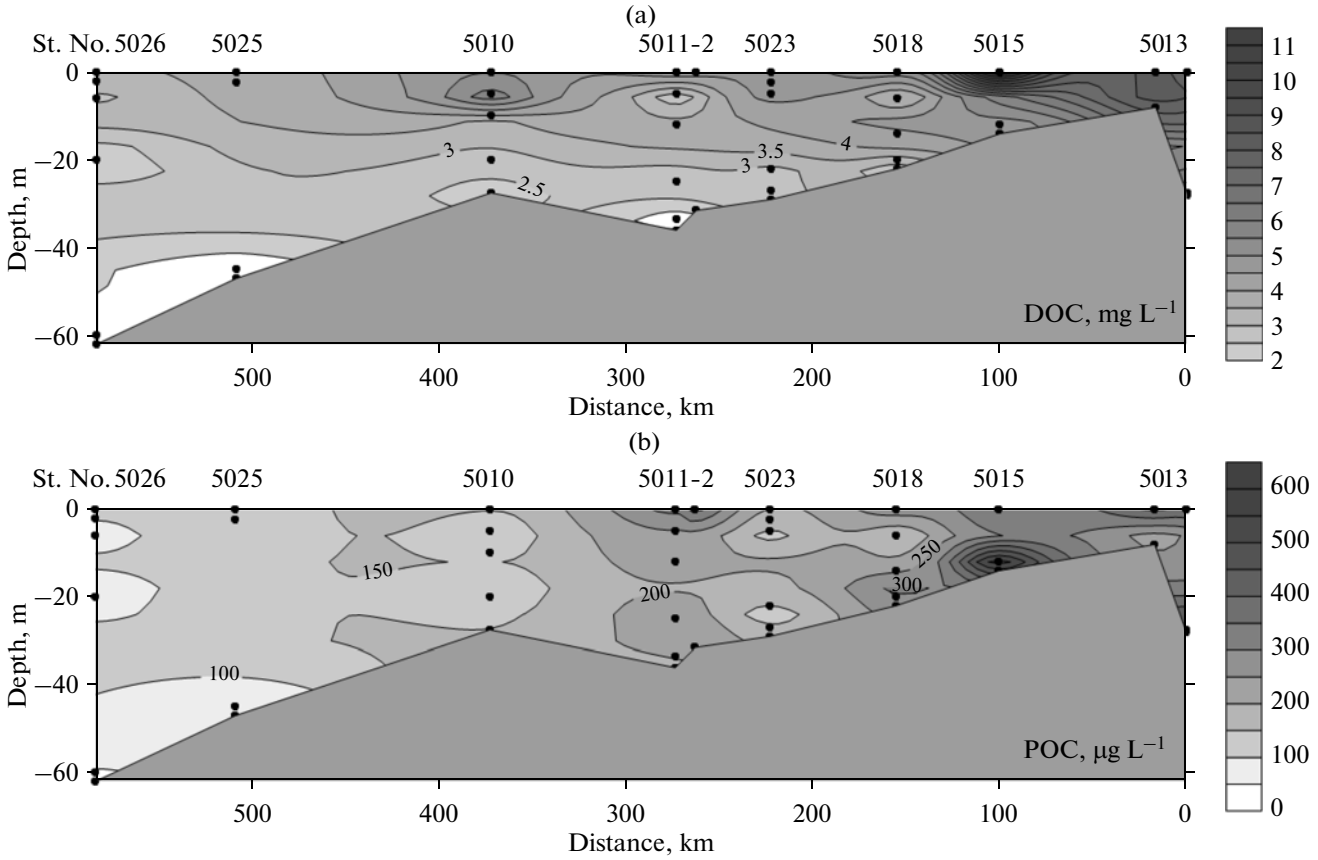

Fig. 2. Distribution of (a) the concentration of the dissolved carbon (DOC) and (b) the particulated C_{org} (POC) in the water column along the southern termination of the meridional profile.

pended particulate matter. The maximal concentrations of the latter were determined in the mouth sites of the profile, where the C_{org} has mainly a terrigenous origin and, respectively, in the surface layer of the water column depleted in ^{13}C down to –30.05‰ (site 5015, Table 1, Fig. 4).

In the water column of the shelf sites (site 5025), the particulate organic matter contains not only terrigenous but also marine (phytoplanktonogenic) OM, which shifts the $\delta^{13}C–CO_{org}$ to higher values (–23 to –24‰) (Fig. 4).

Three frontal zones are distinguished by the distribution of the $\delta^{13}C–POC$: (1) the southernmost zone between sites 5014 and 5013, (2) the zone between sites 5014 and 5018, and (3) from site 5018 to site 5024. The identification of these frontal zones is consistent with the hydrochemical data. In particular, the first zone is characterized by the high content of all the biogenic elements and the decrease of the oxygen content in the suprabottom waters (site 5014). The second zone located downstream the river is less expressed in terms of the hydrochemical parameters and is extended to the southern termination of the profile.

It should be admitted that the sensitivity of the mass-spectrometric isotopic method of the determination of the C_{org} source is higher than the analytical hydrochemical methods. For this reason, the use of the $\delta^{13}C–POC$ is more preferable for distinguishing the frontal zones, because it provides insight into the proportions of the terrigenous (allochthonous) and phytoplanktonogenic (autochthonous) OM in the particulate matter of each of the three distinguished frontal zones.

The values of $\delta^{13}C$ in the bicarbonate-ion dissolved in water. The river waters differ from the seawaters not only in the lowered total alkalinity but also in the isotopic composition of the bicarbonate ion. The values of $\delta^{13}C\text{-}HCO_3^-$ along the profile vary in the surface waters and estuary from –5.92 to –7.49‰, and from –0.98 to –4.06‰ at the seaward sites (Table 2).

The concentration and isotopic composition of the carbon of the bicarbonate ions in the river and estuarian waters primarily depend on the decomposition of the OM in the water by microorganisms with the formation of low-molecular acids and on influx of diverse

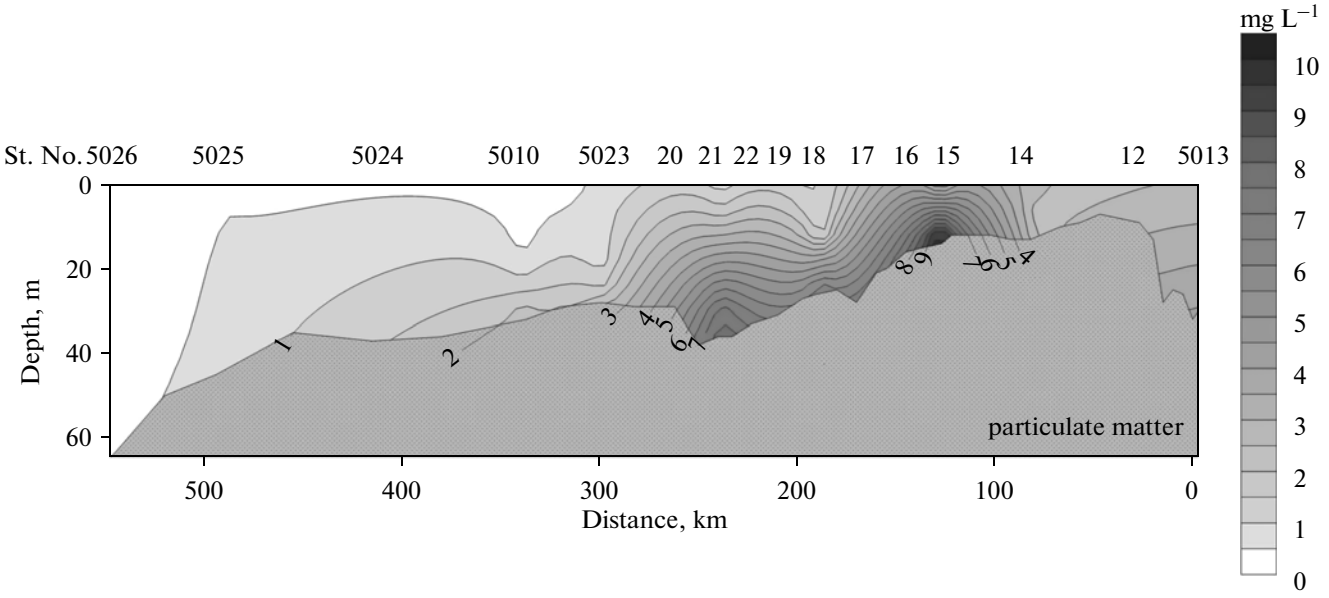

Fig. 3. Distribution of the particulate matter content (mg L^{-1}) in the water column along the southern termination of the meridional profile.

species (dissolved and colloidal) of humic acids from the soil cover of the Yenisei River's drainage area.

Based on the $\delta^{13}C\text{-}HCO_3^-$ in the surface layer of the water column, the river waters were spread up to 76° N in the Kara Sea in September of 2011 (sites 5032 with $\delta^{13}C\text{-}HCO_3^-$ of –4.06‰ in the surface layer; Table 2). It is likely that the desalinated waters did not occur northward of site 5032 in September of 2011.

The methane distribution in the water column. The concentration of methane in the water column of the Kara Sea has been studied since 1993 [3]. The methane concentrations measured in September of 2011 in the surface layer (22.44–83.11 nM) lie within the earlier determined limits (Tables 3, 4). As the salinity and depth increase, the methane concentration decreases to 2.17 nM.

The distribution of methane in the water column along the Yenisei profile reveals the maximum in the area of site 5010 (Fig. 5). In the surface layer of this site, the methane concentration is 83.31 nM (0.0833 μL L^{-1}). One more maximum of the methane concentration was found in the suprabottom layer of site 5018 (89.17 nM or 0.0892 μL L^{-1}) (Table 3).

The isotopic carbon composition of the methane from the surface layer in the area of site 5026 accounted for –69.15‰, which suggests its mostly microbial origination both in the sediments and in the water column, thus confirming the previous conclusions [3, 5, 16, 20, 26].

All the cited authors accept the microbial genesis of the methane in the Holocene sediments and the water column of the Kara Sea in spite of the high hydrocarbon potential of the ancient deposits of this sea and the presence of large hydrocarbon reserves at the Leningradskoe, Rusanovskoe, and other fields.

The integral rate of the microbial processes or the rate of the dark assimilation of carbon dioxide. The rate of the dark $^{14}CO_2$ assimilation in the surface layer of the water column systematically decreases from the south northward from 0.301 μgC L^{-1} day^{-1} (site 5011-2) to 0.009 μgC L^{-1} day^{-1} (site 5039, Table 5) [9].

The DCA value in the suprabottom layer also decreases, while the suprabottom water from the multicorer demonstrates its increase from 1.2 to 6.12 times as compared to the surface layer, which points to the more intense activity of the microorganisms near the water–sediment boundary.

The input of additional sources of reduced compounds (sodium-S thiosulfate and ammonium nitrogen) in experiments with suprabottom water resulted in an increase of the rate of the $^{14}CO_2$ assimilation. This indicates that the suprabottom water contains autotrophic microorganisms, which caused the intense oxidation of reduced compounds supplied from the sediments [9].

An increase in the DCA's intensity was also caused by the addition of ammonium nitrogen in the fluffy layer. At the same time, the input of sodium thiosulfate in the fluffy layer did not affect the DCA's rate. Hence, the number of thionic microorganisms in the studied samples of the fluffy layer is low as compared to the nitirifiers.

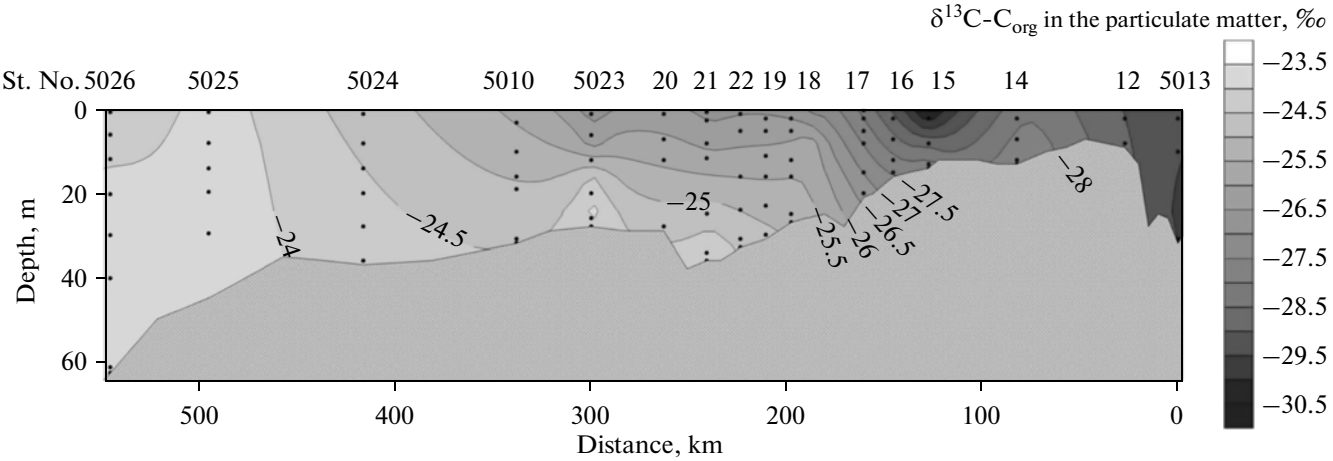

Fig. 4. Distribution of the $\delta^{13}C$–C_{org} (‰) in the particulate matter from the water column along the southern termination of the meridional profile.

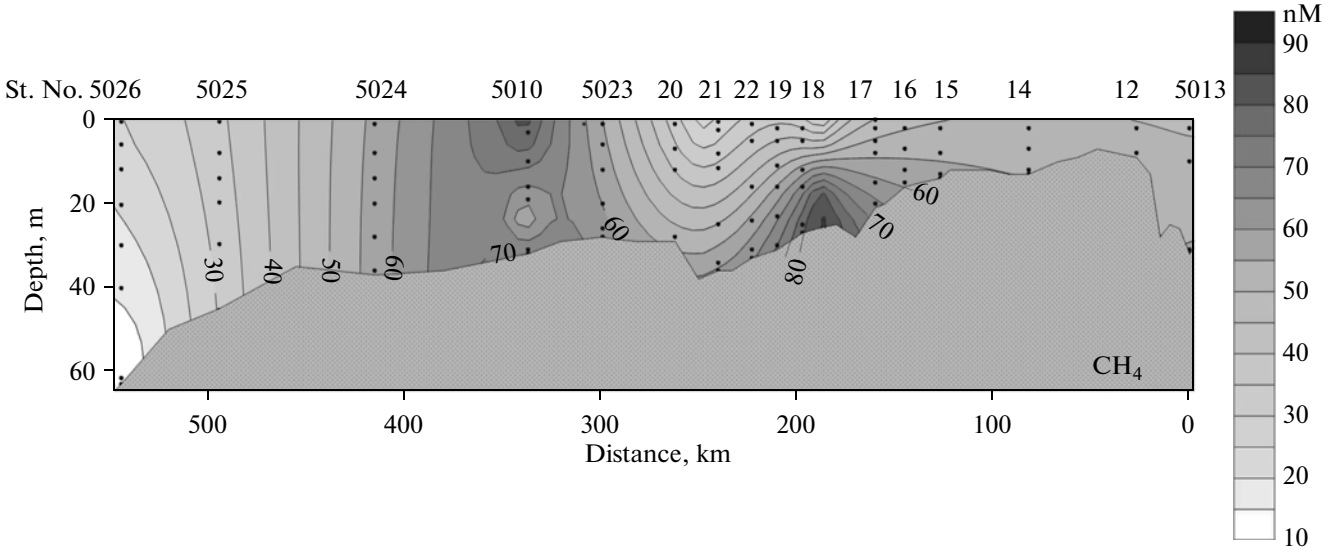

Fig. 5. Distribution of the methane concentration (CH_4, nM) in the water column along the southern termination of the meridional profile.

The total number of microorganisms (TNM) in the water column and the fluffy layer. The value of the TNM in the surface layer of the water column in September of 2011 decreased from the south northward along the meridional profile from 1377 × 10^3 cells mL^{-1} in the Yenisei River's bed (site 5013) to 444 × 10^3 cell mL^{-1} on the outer shelf (site 5033) (Table 6). The values of the TNM in the bottom layer at these sites are 1889 × 10^3 cells mL^{-1} (site 5013) and 233 × 10^3 cells mL^{-1} (site 5033); i.e., the order of magnitude of these values in the bottom layer at these sites remains unchanged as compared to the surface water layer.

In the suprabottom layer of the river bed and the estuary of the Yenisei River, the TNM value remains practically the same as in the surface and bottom layers of the water column (salinity < 15 PSU, sites 5013 and 5011-2, Table 6). With the northward increase in the salinity above 15 PSU, the TNM value in the suprabottom layer increases by 1.3–2.4 times. An especially noticeable growth of this value is observed in the fluffy layer, where the TNM may reach × 10^3 cells cm^{-3} (site 5026), which implies a 32 times increase as compared to the surface layer of the water column and a 17.5 times increase as compared to the suprabottom water. This is accompanied by an increase in the biomass of the heterotrophic and chemoautotrophic microorganisms, i.e., the newly formed C_{org}, in the fluffy layer

2. Brief Characteristics of the Sediments

The profile studied in September of 2001 is subdivided into the following sedimentary facies (from the

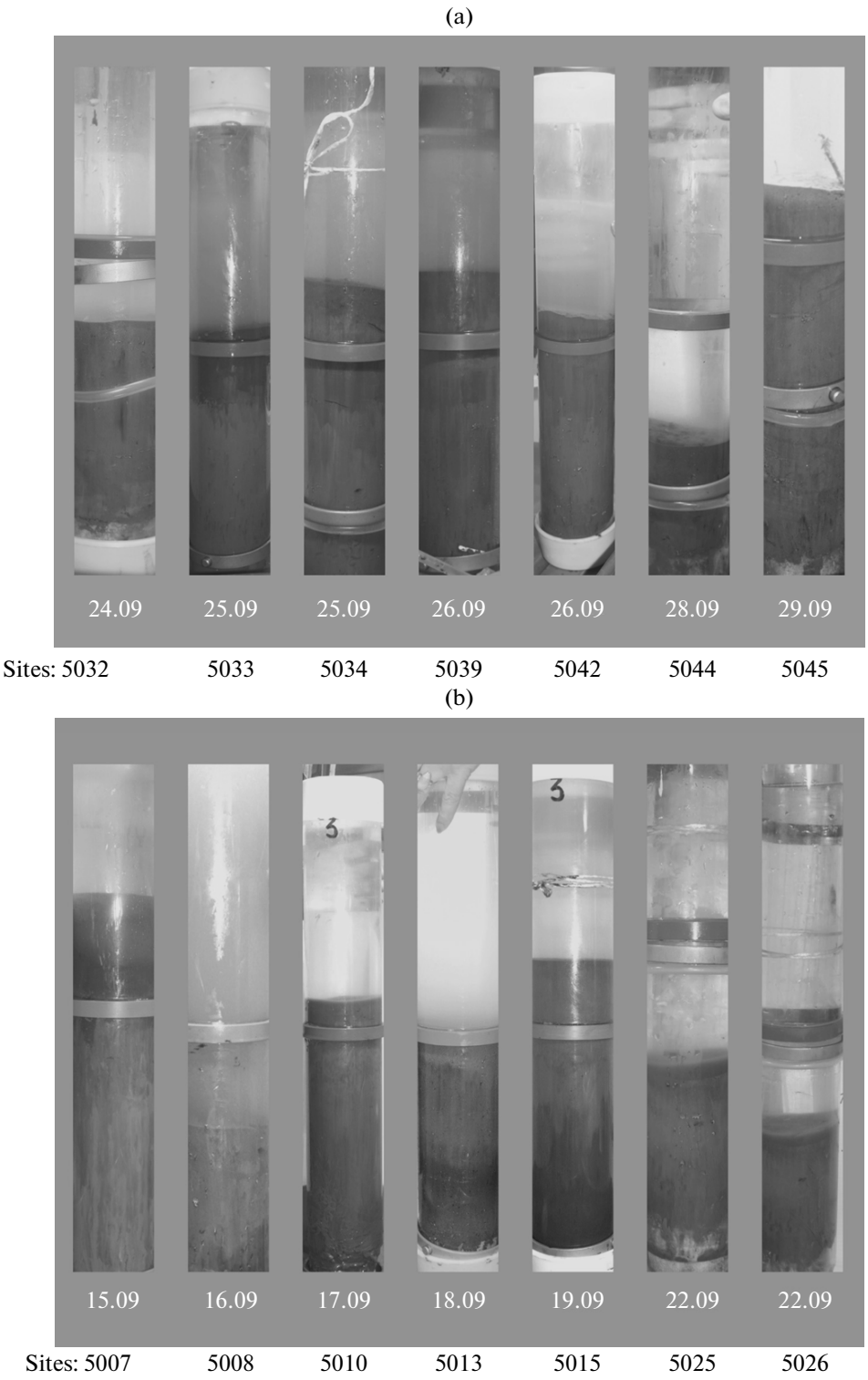

Fig. 6. The studied cores of the multicorer with the samples of the suprabottom water and sediments (a, b) and the surface liquid layer of the sediment–fluffy layer in the multicorer pipe at the sampling sites (c).

south northward): the riverine, the estuarian, the inner and outer shelf, and the deep-water of the St. Anna Trough. The detailed description of these facies was reported in several works with a generalization being in [12]. In our work, our attention is focused on the compositional characteristics of the liquid layer (fluffy

(c)

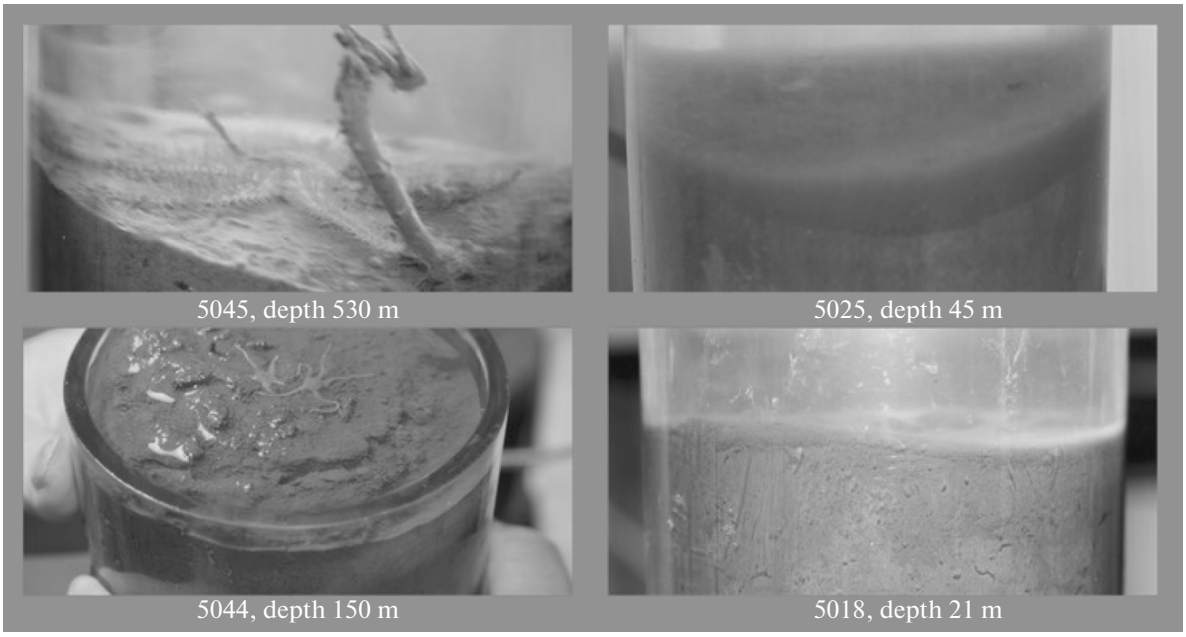

Fig. 6. (Contd.)

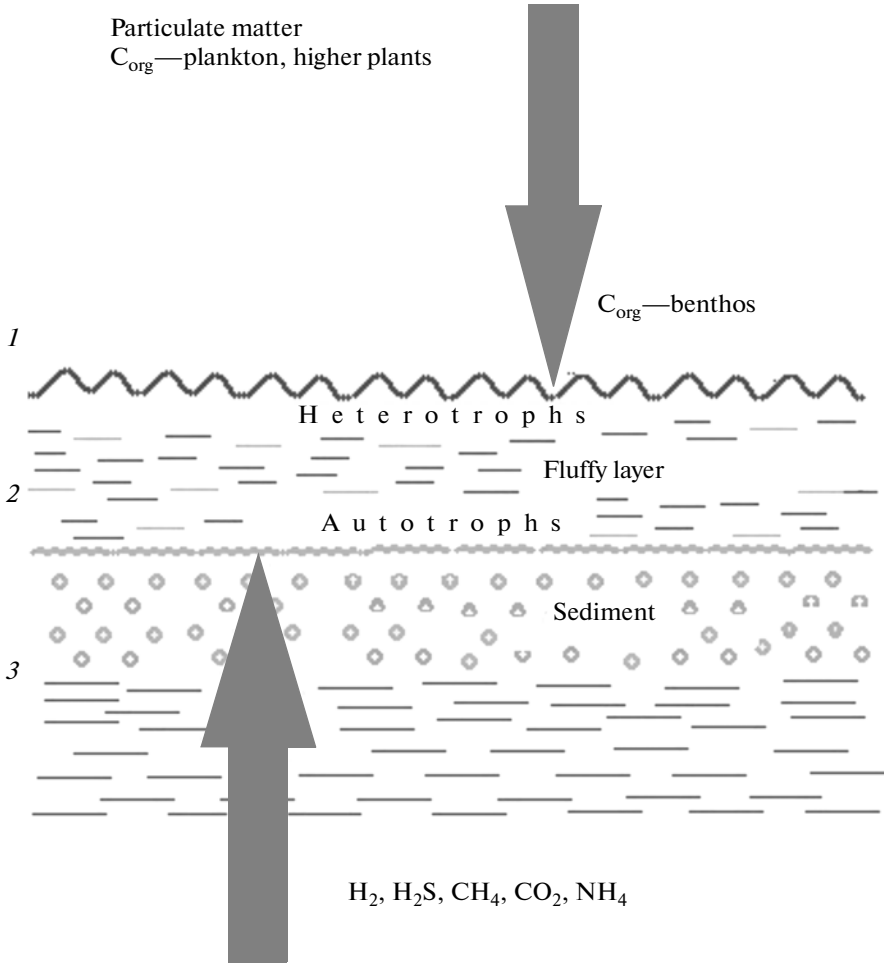

Fig. 7. Structural scheme of the water column–bottom sediment contact zone. The multicorer cores consist of three media: (*1*) the liquid (suprabottom water) with the particulate matter, (*2*) the semiliquid (fluffy layer), and (*3*) the solid (watered surface sediment).

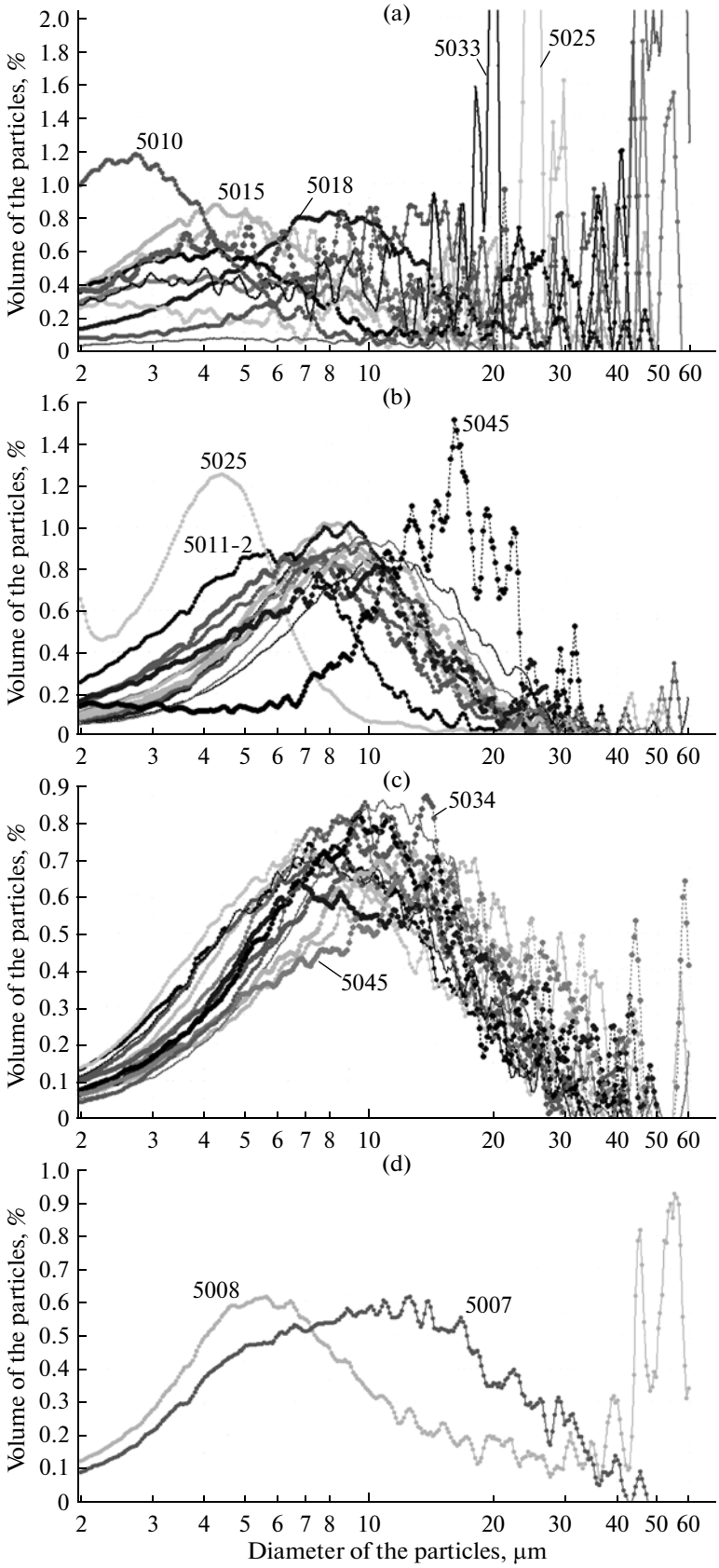

Fig. 8. The differential distribution of the volume contents of the particles: (a–c) near-bottom bathometric samples from the horizon 1–3 m from the bottom; (b) the suprabottom water from the multicorer from the horizon 5–50 cm from the bottom; (c) the fluffy layer from the bottom 1–3 cm; (d) in the upper layer of the bottom sediments from the layer of 0–0.5 cm.

Table 1. Physicochemical parameters of the surface layer (0–5 m) of the water column along the Yenisei River–Kara Sea–St. Anna Trough meridional profile

Site no.	5013	5014	5015	5018	5021	5011-2	5023	5010	5025	5026	5032	5033	5034	5039	5042	5044	5045
Depth, m	30	10	14	22	34	36	29	32	47	66	58	124	222	371	476	158	321
Salinity, PSU	0.069	0.06	0.52	13.3	16.4	13.60	16.6	26.2	22.9	24.1	28.64	27.27	31.24	31.70	32.01	30.89	33.40
Concentration of the particulate matter, mg L^{-1}*	2.55	2.93	2.73	1.15	1.04	1.267	0.82	0.44	0.47	0.34	0.28	0.31	0.26	0.162	0.151	0.35	0.19
Content of C_{org} in the particulate matter, % of the particulate matter**	15	14	13	24	35	n.a.	15	24	25	33	25	26	29	39	44	35	58
DOC, mg L^{-1}**	5.95	8.87	7.35	3.53	n.a.	4.72	4.55	4.94	3.36	3.24	2.24	2.48	n.a.	2.54	3.67	5.81	1.05
$\delta^{13}C$–C_{org} of the particulate matter, ‰***	–29.73	–28.14	–30.05	–27.58	–26.57	–28.46	–26.65	–25.11	–23.70	–25.39	–24.59	–24.47	–23.85	–23.58	–24.01	–24.28	–23.90

Note: n.a. means not analyzed.

* Analyst M.D. Kravchishina.

** Analysts N.A. Belyaev and M.S. Ponyaev.

*** Analyst T.S. Prusakova.

Table 2. Carbon isotopic composition of the dissolved bicarbonate in the water column of the Kara Sea

Site no.	Horizon, m	Alk*, mg–equiv. L^{-1}	$\delta^{13}C–C_{HCO_3^-}$, ‰
Ob–Yenisei shoal			
5008	2.0	1.556	n.a.
	20.0	2.242	n.a.
	Suprabottom water (0.05 from the bottom)	2.405	–8.67
Yenisei River: river bed, estuary, inner shelf			
5010	3.0	2.067	–7.49
	27.0	2.298	–3.33
	Suprabottom water (0.02 from the bottom)	2.505	–6.23
5013	2.0	1.069	n.a.
	31.0	1.045	–3.73
5018	2	1.516	–5.94
	21	2.250	–6.08
	Suprabottom water (0.02 from the bottom)	2.226	–5.67
5011-2	0.5	1.660	n.a.
	32.2	2.314	–3.11
	Suprabottom water (0.02 from the bottom)	n.a.	–2.91
5023	1.0	1.588	n.a.
	26.0	2.274	n.a.
	Suprabottom water (0.02 from the bottom)	2.298	–6.67
5026	0.5	1.963	–5.92
	62.0	2.370	–6.81
	Suprabottom water (0.01 from the bottom)	2.405	–4.98
Outer shelf–St. Anna Trough–East			
5032	1.0	2.135	–4.06
	57.0	2.378	–2.45
5033	2.0	2.059	–1.29
	122.0	2.382	–2.19
	Suprabottom water (0.01 from the bottom)	2.366	–1.56
5034	Suprabottom water (0.03 from the bottom)	n.a.	–2.04
5039	1.0	2.250	–0.98
	358.0	2.394	–1.69
	Suprabottom water (0.05 from the bottom)	2.390	–1.20
5042	1.0	2.258	–1.16
	465.0	2.402	–3.67
	Suprabottom water (0.05 from the bottom)	2.390	–1.81
5044	1	2.234	–1.31
	154.0	2.402	–3.87
	Suprabottom water (0.01 from the bottom)	2.406	–2.30
5045	1.0	2.330	–2.48
	526.0	2.410	–1.87
	Suprabottom water (0.01 from the bottom)	2.404	–2.11

Note: n.a. means not analyzed.

* Data of P.N. Makkaveev.

Table 3. Concentration of methane in the water column of the Kara Sea

Site no.	Horizon	Horizon, m	CH_4, nM
Yenisei River: river bed, estuary			
5010	surface	0.02	83.31
	near-bottom	27.5	51.12
	suprabottom	0.4 (from the bottom)	78.05
5013	surface	0.0	49.37
	near-bottom	27.5	53.46
	suprabottom	0.4 (from the bottom)	55.22
5018	surface	0.0	23.03
	near-bottom	20.0	89.17
	suprabottom	0.3 (from the bottom)	85.65
5011-2	surface	0.0	22.44
	near-bottom	37.0	58.14
	suprabottom	0.4 (from the bottom)	62.83
5026	surface	2.0	25.43
	near-bottom	60.0	11.32
	suprabottom	0.6 (from the bottom)	13.08
Outer shelf–St. Anna Trough			
5032	surface	1.5	3.85
	near-bottom	56.0	20.76
	suprabottom	0.5 (from the bottom)	19.65
5033	surface	2.5	6.22
	near-bottom	120.0	31.86
	suprabottom	0.3 (from the bottom)	31.27
5039	surface	1.0	6.69
	near-bottom	355.0	3.99
	suprabottom	0.3 (from the bottom)	4.57
5042	surface	1.0	2.17
	near-bottom	460.0	1.76
	suprabottom	0.3 (from the bottom)	3.52
5044	surface	2.0	2.40
	near-bottom	147.0	2.58

layer) 0.0–0.5 cm above the surface sediment horizon (0.5–2 cm). The sampling of the sediments by heavy geological devices (bottom grabbers, box corers, and pipes) usually leads to the disintegration of the surface sediment layer. For this reason, the structure of the water–sediment contact zone has not yet been studied in detail. We attempted to fill this gap.

The structure of the water–sediment contact zone was studied in cores taken using a multicorer. The contact zone consists of three subzones: the suprabottom water, the fluffy layer (≥90% moisture), and the surface sediment (≤90% moisture) (Fig. 6). Figure 7 demonstrates the structure of the water–sediment contact. The particulate organic matter supplied into the contact zone from the top is represented by allochthonous (terrigenous) matter in the form of the remains of higher plants, the products of abrasion, and others and autochthonous (phytoplanktonogenic) matter. The organic matter of the particulates provides for the vital activity of the heterotrophic microorganisms in the suprabottom water, the fluffy layer, and the sediment. The reduced compounds supplied into the suprabottom water from the sediments serve as an energetic substrate for the autotrophic bacteria and archea.

The distribution of the grain-size composition of the particulates at the water–sediment boundary. The grain-size composition of the particulates may be a

Table 4. Concentration of methane in the surface horizon of the water column of the Kara Sea according to the observations of 1995–2011

Area	Ranges of the CH_4 concentration, $\mu L\ L^{-1}$	Number of samples	Average CH_4 concentrations		References
			μL^{-1}	nM	
Yenisei R., bed	0.51–4.37	15	1.51	67.4	[3]; [5]; This work
Yenisei R., estuary	0.05–1.87	12	0.66	29.5	
Shelf in the area of the Yenisei R.'s emptying	0.4–1.49	9	0.69	30.8	[5]; This work
Ob R., bed	0.05–3.20	15	1.24	55.4	[3]; [5]; [26]
Ob R., estuary	0.40–0.50	4	0.41	18.3	[5]; [26]
Shelf in the area of the Ob R.'s emptying	0.25–0.46	13	0.40	17.9	
Other areas of the Kara Sea's shelf	0.18–1.1	11	0.53	23.9	[3]; [26]

Table 5. Rate of the dark $^{14}CO_2$ assimilation ($\mu gC\ L^{-1}\ day^{-1}$) in the water column and the fluffy layer

Sites Water layer	5045	5044 **	5042	5039	5033	5010 *	5011-2	5018	5007
Surface	0.017	0.014	0.014	0.009	0.017	0.088	0.301	0.263	0.064
Near-bottom	0.009	0.013	0.011	0.010	0.005	0.141	0.277	0.238	0.060
Suprabottom	0.099	0.017	0.066	0.012	0.104	0.203	0.352	0.420	0.153
Fluffy layer	2.324	1.504	n.a.	0.114	0.384	0.679	3.911	0.749	n.a.

Note: The added components: N—ammonium nitrogen, S—sodium thiosulfate.
* The suprabottom water + N = 0.234 $\mu gC\ L^{-1}\ day^{-1}$.
The suprabottom water + S = 0.311 $\mu gC\ L^{-1}\ day^{-1}$.
** The fluffy layer + N = 1.580 $\mu gC\ L^{-1}\ day^{-1}$; the fluffy layer + S = 1.440 $\mu gS\ L^{-1}\ day^{-1}$.

sensitive indicator of the matter transformation at the water–sediment contact [34]. According to the grain-size data, the average size of the particulates in the suprabottom water is 8.1 μm.

In the suprabottom water of the river and estuarian sites, 67 to 97.4% of the particulates vary in size within 2–10 μm. We may suggest that the coarsening of the particulates that compose the fluffy layer is related not only to the physicochemical processes but also to the formation of the organomineral particles at the expense of the increase of the C_{org}, including the biomass of the microorganisms, in the fluffy layer as compared to the particulates in the suprabottom water.

The low average content of the pelitic particles (53.7–63.6%) at the shelf site may be related to the lower content of C_{org} relative to the sites at the Yenisei River's bed and the estuary.

The suprabottom water and the fluffy layer from the sites in the St. Anna Trough are heterogeneous in their grain size composition. The amount of pelitic particles

Table 6. Total number of microorganisms (10^3 cells mL^{-1}) in the water column and the fluffy layer

Sites Water layer	5013	5018	5011-2	5010	5026	5032	5033	5039	5042	5044	5045	5007	5008
Surface	1377	n.a.	1583	407	543	309	444	322	145	253	159	664	1924
Near-bottom	1889	853	823	516	233	283	233	49	44	47	56	280	853
Suprabottom	1750	n.a.	1100	850	1000	950	600	400	350	320	300	500	2500
Fluffy layer	10930	69781	25173	n.a.	17511	n.a.	6097	9662	9720	17793	n.a.	13223	n.a.

Note: n.a. means not analyzed.

Table 7. Chemical composition (%) of the fluffy layer and the surface sediments of the river facies along the Yenisei profile. Siliceous diatomaceous–clayey from gravel–sandy to silty–pelitic sediments

Sites Horizon	SiO_2	Al_2O_3	Fe_2O_3	TiO_2	MnO	MgO	CaO	Na_2O	K_2O	P_2O_5	Ba	Co	Cr	Ni	Sr	Cu	Zn	S	L.O.I.
5013 Fluffy layer	73.56	9.96	4.04	0.53	0.08	1.39	2.48	1.78	1.55	0.15	0.044	0.0018	0.0139	0.0044	0.0255	0.0015	0.005	0.070	12.5
5013 1–5 cm	78.20	8.71	3.08	0.46	0.05	1.00	2.28	1.88	1.57	0.10	0.044	0.0016	0.0055	0.0025	0.0225	0.0009	0.0039	0.060	10.8
5014 Fluffy layer	64.92	12.96	5.69	0.75	0.20	1.90	3.53	2.15	1.78	0.19	0.050	0.0026	0.0086	0.0041	0.0359	0.0019	0.0064	0.050	5.7
5014 0.5–2 cm	67.10	12.21	5.27	0.67	0.15	1.54	3.43	2.18	1.73	0.15	0.042	0.0023	0.0072	0.0040	0.0345	0.0016	0.0058	0.030	5.4
5015 Fluffy layer	51.23	14.59	8.59	0.81	0.32	2.61	2.28	3.05	1.65	0.23	0.028	0.0028	0.0094	0.0069	0.0215	0.0043	0.0095	0.110	14.4
Fluffy layer average (3)	63.24	12.50	6.11	0.70	0.20	1.97	2.76	2.32	1.66	0.19	0.041	0.0024	0.0106	0.0051	0.0276	0.0026	0.0070	0.077	10.86
Sediment average (2)	72.62	10.46	4.17	0.56	0.10	1.27	2.85	2.03	1.65	0.12	0.043	0.0018	0.0063	0.0032	0.0285	0.0033	0.0048	0.045	8.1
Average composition* (8)	68.01	11.94	5.8	0.79	0.18	1.53	1.33	1.52	2.26	0.20	0.051	0.0017	0.0065	0.0042	0.0173	0.0120	0.0070	0.040	n.a.

Note: Tables 7–10 list the X-ray fluorescence data. The analyst was T.G. Kuz'mina (Vernadsky Institute of Geochemistry and Analytical Chemistry of the Russian Academy of Sciences).
* Data after [12]; n.a. means not analyzed. L.O.I.—Losses on ignition.

Table 8. Chemical composition (%) of the fluffy layer and the surface sediment horizon (0.5–2 cm) in the estuary zone. Finely dispersed olive-gray and/or black pelitic mud and silty sandy clay

Site	Horizon	SiO_2	Al_2O_3	Fe_2O_3	TiO_2	MnO	MgO	CaO	Na_2O	K_2O	P_2O_5	Ba	Co	Cr	Ni	Sr	L.O.I.
5018	Fluffy layer	49.19	14.88	9.46	0.75	0.73	2.59	1.79	3.36	1.71	0.28	0.024	0.0026	0.0083	0.0063	0.0189	15.1
	Sediment	49.84	14.93	9.97	0.73	0.70	2.64	1.72	3.43	1.70	0.29	0.026	0.0025	0.0081	0.0066	0.0181	15.2
Average composition* (32 samples)	Sediment	53.73	12.77	8.05	0.82	0.42	2.96	1.95	4.26	2.04	0.28	0.036	0.0024	0.0075	0.0046	0.0214	n.a.

Note: n.a. means not analyzed. L.O.I.—Losses on ignition.
* Data after [12].

Table 9. Chemical composition (%) of the fluffy layer and the surface sediments of the inner shelf. Sands, silts, and sandy–silty–pelitic muds

Sites	Horizon	SiO_2	Al_2O_3	Fe_2O_3	TiO_2	MnO	MgO	CaO	Na_2O	K_2O	P_2O_5	Ba	Co	Cr	Ni	Sr	L.O.I.
5010	Fluffy layer	53.94	14.21	8.85	0.64	0.44	2.08	1.3	3.52	1.91	0.35	0.036	0.0025	0.008	0.0051	0.0178	12.5
	Sediment	56.29	14.60	7.89	0.65	0.09	2.04	1.22	3.58	2.13	0.20	0.031	0.0023	0.009	0.0052	0.0168	10.8
5025	Fluffy layer	70.13	9.54	3.97	0.51	0.27	0.91	1.19	2.39	1.79	0.11	0.037	0.0012	0.0056	0.0024	0.0165	9.0
	Sediment	75.72	9.70	2.98	0.50	0.21	0.94	1.32	2.45	2.22	0.14	0.058	0.0012	0.0050	0.0022	0.0210	3.6
Average composition* (19–26 samples)	Sediment	67.27	10.12	5.05	0.66	0.34	1.83	1.51	3.32	2.18	0.18	0.0516	0.0019	0.0052	0.0059	0.0243	n.a.

Note: n.a. means not analyzed. L.O.I.—Losses on ignition.
* Data after [12].

2–10 μm in size in the suprabottom water of the trough varies within wide ranges from 23.8 to 67%. In the trough, the "normal" sedimentation was disturbed by the influx of slope material, which determined the variable size of the particulates and the different content and composition of the OM in the suprabottom water.

The grain-size composition of the fluffy layer may strongly differ from the size of the particulates in the suprabottom water (Fig. 8). The content of the pelitic fraction in the fluffy layer varies from 38 to 75%. All the differential distributions of the grain-size composition of the fluffy layer (by volume) are characterized by the absence of particle sorting (S_o) and an expressed size extremum. The median diameter (Md) of the fluffy layer varies from 7 to 13 μm. The differential curves form a mode in the transitional area between the pelitic (particles <10 μm) and the silty (particles of 10–100 μm) fractions.

All these facts indicate that the dispersed system of the fluffy layer is aggregately unstable. The newly formed OM (microbial biomass) in this layer provides

Table 10. Chemical composition (%) of the fluffy layer and the surface sediments of the outer shelf. Brown and dark brown pelitic muds with a sandy–silty admixture

Sites	Horizon	SiO_2	Al_2O_3	Fe_2O_3	TiO_2	MnO	MgO	CaO	Na_2O	K_2O	P_2O_5	Ba	Co	Cr	Ni	Sr	L.O.I.
5026	Fluffy layer	59.69	14.05	5.97	0.62	0.53	1.71	1.56	3.64	2.13	0.20	0.043	0.0025	0.0082	0.0041	0.0212	9.6
	Sediment	62.99	13.26	5.71	0.62	0.49	1.58	1.58	3.16	2.17	0.19	0.046	0.0027	0.0069	0.0037	0.0198	8.0
5032	Fluffy layer	70.4	12.04	4.01	0.60	0.09	1.26	1.69	2.68	2.17	0.15	0.056	0.0016	0.0074	0.0027	0.022	4.5
5034	Sediment	55.6	16.00	7.61	0.70	0.60	2.12	0.96	2.95	2.39	0.28	0.061	0.0038	0.0097	0.0059	0.0168	10.5
Average composition* (11 samples)	Sediment	57.17	11.32	6.94	0.62	1.17	2.24	1.23	4.66	2.29	0.42	0.466	0.002	0.0040	0.0040	0.0182	n.a.

Note: n.a. means not analyzed. L.O.I.—Losses on ignition.
* Data after [12].

Table 11. Changes in the titanium (Al_2O_3) and alumina (SiO_2/Al_2O_3) modulus in the fluffy layer and the surface sediment of different facies

Facies	Site no.	Horizon	Al_2O_3/TiO_2	SiO_2/Al_2O_3
River	5013	Fluffy layer	18.79	7.38
		Sediment	18.93	8.98
	5014	Fluffy layer	17.28	5.00
		Sediment	18.22	5.49
	5015	Fluffy layer	18.01	3.51
Estuarian	5018	Fluffy layer	19.84	3.30
		Sediment	20.45	3.27
Inner shelf	5010	Fluffy layer	22.20	3.79
		Sediment	22.46	3.85
	5025	Fluffy layer	18.70	7.35
		Sediment	19.40	7.81
Outer shelf	5026	Fluffy layer	22.66	4.25
		Sediment	21.38	4.75

for the intensification of the coagulation and flocculation. The rate of the coagulation of the submicron and pelitic particles is orders of magnitude higher than that of the aggregation of the coarser particles [32]. The difference in the rates presumably results in the flattening of the differential curves of the grain-size composition.

The upper layer of the bottom sediments (0–0.5 cm) may inherit the grain-size composition from the fluffy layer. The formation of the grain-size composition of the surface sediments is not terminated at this stage.

The chemical composition of the fluffy layer and the surface sediments. The fluffy layer and the surface layer of the alluvium from the deepening in the river bed (site 5013) are represented by greenish and yellowish brown fine to medium grained sand with an admixture of pelitic material, plant detritus, and shell fragments. The values of the Eh = +100 to −140 mV. An H_2S smell occurred in the sediments from the horizon of 1.0–5.0 cm.

In the main river bed (sites 5014 and 5015), the alluvial sediments vary in their grain size composition from sands to pelitic muds. The moisture of the sands and the pelitic muds is 32.7 and 68.4%, respectively.

The chemical composition of the fluffy layer and the surface horizon is dominated by SiO_2 and Al_2O_3 (Table 7). The sediment has a 2–5% higher SiO_2 content and somewhat lowered contents of Al_2O_3, Fe_2O_3, and MgO as compared to the fluffy layer, presumably due to the chemical variations in the seasonal fluxes of the particulate matter (spring–summer–autumn).

The average chemical composition of the fluffy layer and the surface sediments falls within the limits typical of the river facies of the Yenisei River (Table 7).

The fluffy layer (Eh = +160 mV) in the estuary (site 5018) consists of yellowish brown silt and pelite. The sediment (Eh = +100 mV) is represented by finely dispersed pelitic mud with an admixture of olive gray silty-sandy material with black films of hydrotroilite (Table 8). The moisture of the sediments from the horizon of 0.5–2 cm is close to 60%.

As compared to the surface sediment in the estuary, the fluffy layer is higher in Fe_2O_3 and MnO and lower in SiO_2 and Al_2O_3 (Table 8). Site 5018 is located in the zone of the precipitation of a tremendous amount of clay and some authigenic minerals from the water suspension in response to the mixing between the river and sea waters. In this area, the clay particles change their charge. As compared to the sediments of the river facies in the fluffy layer and the sediments of the estuarian facies, the SiO_2 content decreases by 10–15%, while the content of the components involved in the clay minerals (Al_2O_3, Fe_2O_3, MgO, and others) increases (Table 8).

The fluffy layer and the surface horizon of the deposits of *the inner shelf* (sites 5010 and 5025), unlike the estuary, contain inequigranular material: from sands to pelites. This results in a difference between the chemical compositions of the sediments: the sands and silts have a higher SiO_2 content (70–75%) than the pelitic varieties (54–56%, Table 9).

The surface layer of the sediment contains numerous Polychaeta tubes. The sediments are bioturbated.

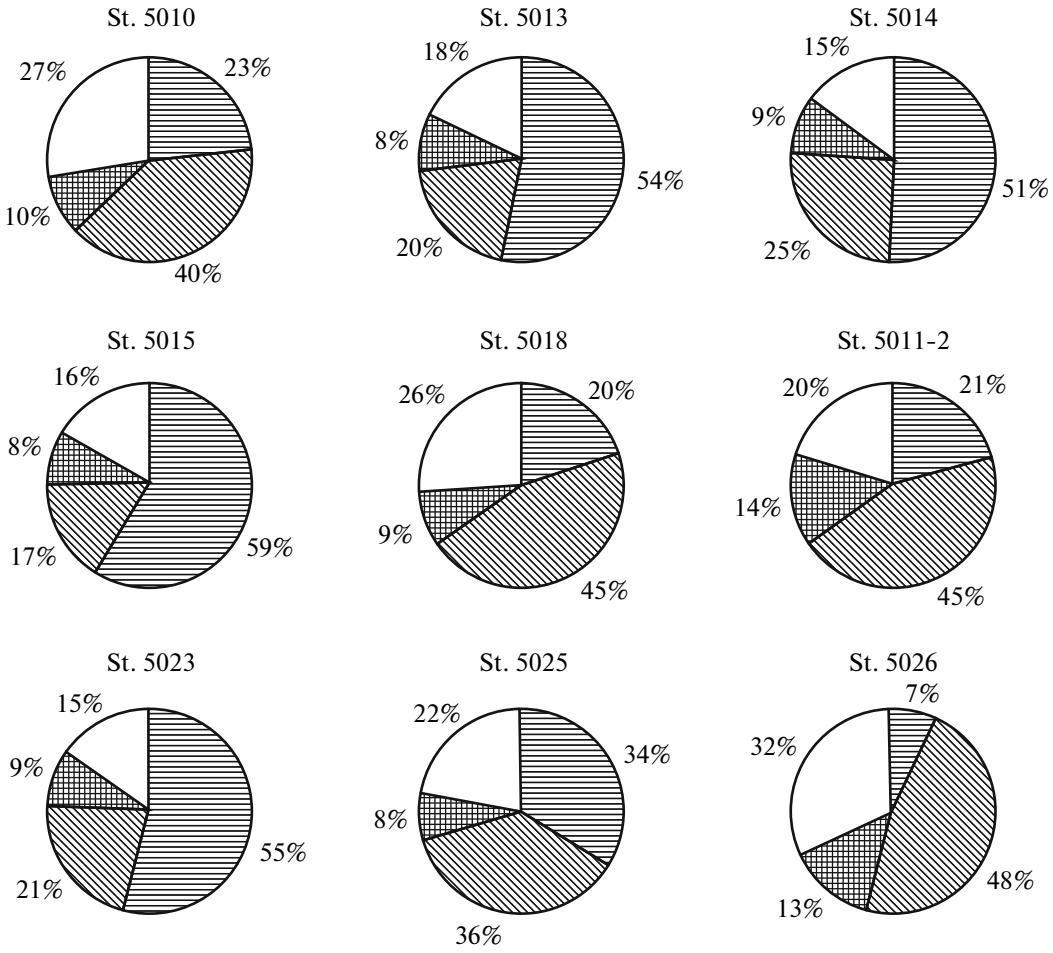

Fig. 9. Content and composition of the clay minerals in the fluffy layer: (*1*) montmorillonite; (*2*) illite; (*3*) kaolinite; (*4*) chlorite.

Below 2 cm, they are weakly reduced (Eh = –40 mV) and contain films of hydrotroilite.

The fluffy layer and the surface sediments of the *outer shelf* facies (site 5026) consist of brown and dark brown pelitic muds with an admixture of sandy-silty material. The fluffy layer has a lower SiO_2 content and higher Al_2O_3, Fe_2O_3, and MgO than the sediments (Table 10). The sediments of the outer shelf are characterized by their elevated contents of MnO, Na_2O, K_2O, and P_2O_5 as compared to the sediments of the previously considered facies (Tables 7–10), which is related to their high positive redox potential (Eh from +100 to +140 mV).

The slight increase of the titanium and aluminum modulus in the sediments relative to the fluffy layer in all the facies (besides the outer shelf facies) indicates an increase of the clastic component in the sediments (Table 11).

Due to the high bioturbation, the sediments of all four facies have oxidized brown surface layers that penetrate the underlying gray reduced muds along the channels of large polychaetes. Below 8 cm, the sediments in the core from the St. Anna Trough (site 5042) change their Eh to negative values.

The distribution and composition of the clay minerals in the fluffy layer and the surface sediment horizon. Selected material was studied using an automated DRON-2.0 diffractometer with K_α irradiation and a graphite monochromator (40 kV, 40 mA).

The x-ray powder diffraction data (Table 12) allowed us to reveal the tendencies in the distribution of the clay minerals in the surface layer of the bottom sediments along the meridional profile.

A stable montmorillonite–illite–kaolinite–chlorite association [7] is traced from the south northward: from the Yenisei River's bed (sites 5013, 5014, and 5015) further into Yenisei Bay (sites 5018 and 5011-2) and the shelf zone (sites 5023, 5025, 5026, 5032, and 5033) up to the slope of the St. Anna Trough. This zone is characterized by the gradual decrease of the montmorillonite content both in the fluffy layer and in the surface layer of the sediments (Figs. 9, 10). The

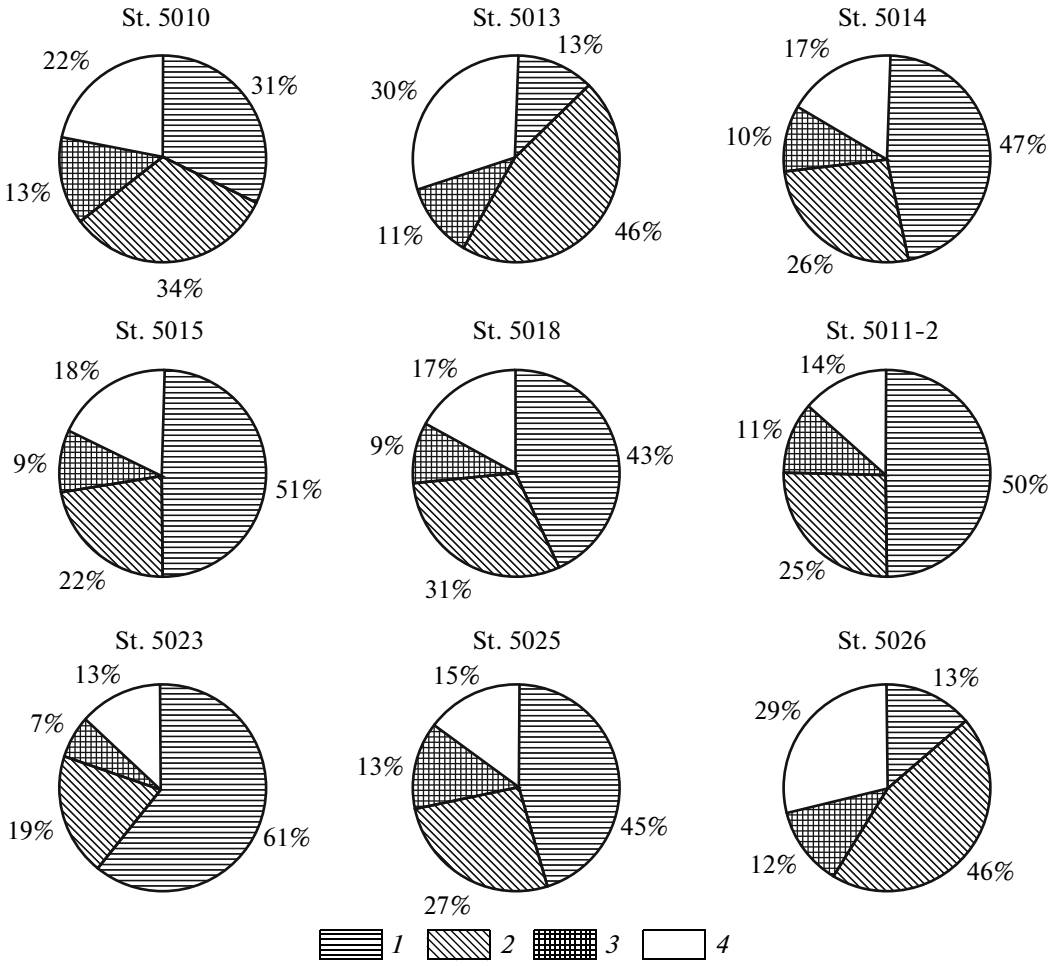

Fig. 10. Content and composition of the clay minerals in the surface sedimentary layer. The symbols are shown in Fig. 9.

slope of the St. Anna Trough (site 5034) shows a sharp decrease in the content of montmorillonite and the change of the above association into kaolinite–chlorite–illite in its fluffy layer (Fig. 11). At the same time, trace amounts of montmorillonite were identified in the surface layer. Clastic material is supplied into the St. Anna Trough from the Frantz Josef Land Novaya Zemlya archipelagos and the North Kara Rise [12]. The influence of such distal sources as the Ob and Yenisei rivers is less significant.

The contents of kaolinite (4–28%), chlorite (13–44%), and illite (17–27%) in the studied area vary in broad ranges. However, the associations of these minerals with relatively stable proportions show a patchy distribution, which can be explained by the influence of the complex hydrodynamic processes in the relatively shallow basin [17].

Contrasting facies patterns determined by the montmorillonite are observed in the barrier mixing zone of the fresh and river waters with the saline seawaters in the Yenisei River's bed. Dioctahedral smectites, including montmorillonite, are formed as three-layer (tetrahedral–octahedral–tetrahedral) sheets with interlayer hydrated exchange cations (Na^+, K^+, Mg^{2+}, and Ca^{2+}), which regulate the degree of intracrystalline swelling of the smectites. This, in turn, affects their diffraction pattern: the *001* basal reflection of montmorillonite with Na^+ and K^+ exchange cations corresponds to interplanar spacing ~12.4 Å, while the substitution of cations by Mg^{2+} and Ca^{2+} leads to the increase of d up to 15.5 Å. The studied material is subdivided into two groups. The montmorillonites from the fresh-water (0.06–0.07‰) surface sediments have $d \sim 14.4$ Å, while those from the saline waters (0.52–33.4‰) have $d \sim 12.6$ Å. This criterion makes it possible to estimate the conditions of the sedimentation.

The content and isotopic composition of the C_{org} in the suspended particulate matter from the water column and in the water–sediment boundary zone. The particulate matter of the surface waters shows the systematic distribution of the C_{org} content from the river

Table 12. Content* (%) of clay minerals in the fluffy layer and the surface horizon of the sediments along the meridional profile

Sites	Montmorillonite		Illite		Kaolinite		Chlorite	
	fluffy layer	sediment	fluffy layer	sediment	fluffy layer	sediment	fluffy layer	sediment
5010	23	31	39	33	10	13	27	22
5013	53	13	20	45	8	11	18	30
5014	51	46	25	26	9	10	15	17
5015	59	49	17	22	8	9	16	18
5018	19	43	42	31	8	9	24	17
5011-2	21	51	44	26	14	11	20	14
5023	54	59	21	19	9	7	15	13
5025**	9/41	45	44/30	27	9/11	13	26/18	15
5026	7	13	47	45	13	12	32	28
5032	10	19	41	28	10	28	37	23
5033	traces	18	50	49	10	11	29	21
5034	traces	1	50	57	6	5	44	37
5039	traces	2	61	72	6	8	32	17
5042	traces	2	55	56	15	12	29	29
5044	traces	1	60	62	4	5	35	31
5045	traces	5	56	52	12	14	32	29

* Analyst O.M. Dara (Shirshov Institute of Oceanology of the Russian Academy of Sciences), DRON-20 diffractometer.
** The fluffy layer is subdivided into two layers.

bed into the open sea via the transitional zone with variable salinity (Table 1). The river water is dominated by terrigenous organic matter depleted in ^{13}C, which is the first end member of the isotopic composition of the C_{ogr}. The particulate matter of the open sea surface waters contains mainly autochthonous organic matter with a heavier isotopic composition. This is the second end member of the series. In other words, the tendency known since 1993 was observed in September of 2011: the C_{org} in the particulate matter of the surface layer of the water column of the Kara Sea along the river–sea profile shows a shift to the heavier isotopic composition [5, 16, 26]. In September of 2011, the runoff of fresh water was recognized up to at least 76° N on the basis of the isotope data (Table 13).

Along the vertical section of the water column (from the top to the bottom) from the water–atmosphere to the water–bottom boundary, the particulated C_{org} is gradually enriched in heavy isotopes, which is especially noticeable from the value of $\delta^{13}C$–C_{org} in the fluffy layer (by 1–3‰ and more). This phenomena was noted by us for the first time in 1993 [16] and considered in more detail in [10, 13, 14].

It was concluded in the cited works on the basis of the microbiological, radio, and stable isotope data that the microbial community of the heterotrophic and hemoautotrophic microorganisms with biomass isotopically heavier than that of the particulate OM ($\delta^{13}C = -20‰$) is developed at the water–sediment boundary in the fluffy layer owing to the supply of phytolanktonogenic OM from above and reduced compounds from below [10]. The abundant development of microorganisms in the fluffy layer follows from the microbiological studies (Table 6), which confirm the large values of the integral rate of the dark CO_2 assimilation (Table 5).

The distribution and composition of the n-alkanes in the fluffy layer and the surface horizon of the sediments. The use of the distribution of the normal alkanes (n-alkanes) as indicators of the terrigenous and planktonogenic inputs in the genesis of the organic matter in the bottom sediments of the northern seas began in the terminal 1970s [25]. Based on the com-

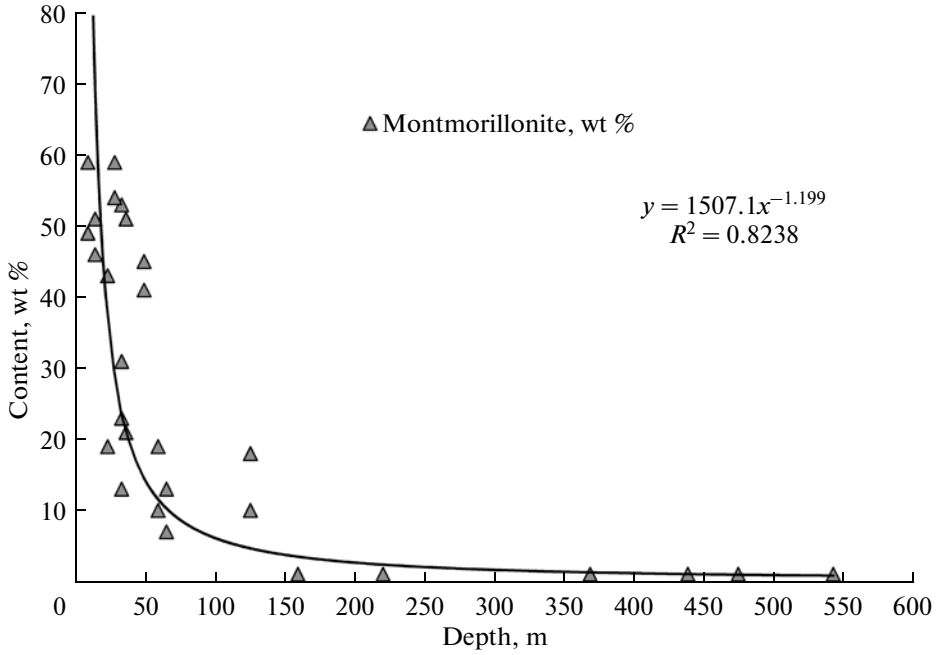

Fig. 11. Change of the montmorillonite content (wt %) in the surface sedimentary layer.

plex analysis of the organic biomarkers, the authors of the cited work distinguished three characteristic geochemical types of OM. The OM of type I formed by the remains of hydrobionts is characterized by the predominance of short-chain alkanes with molecular weight of C17–C19. The terrigenous organic matter of type III has an elevated content of high-molecular n-alkanes C25–C31 with the distinct predominance of odd alkanes. The type-II OM of mixed microbial–terrigenous genesis is characterized by its relatively even distribution with the predominance of C19–C25 maximums and the less expressed predominance of odd peaks. This type of OM rarely occurs in the studied area. The works on studying the molecular composition of the hydrocarbons (HC) of the Kara Sea were continued by Russian and foreign researchers [2, 5, 8, 21, 35, 39].

According to [39], the surface sediments of the Kara Sea, especially in the estuary of the Ob and Yenisei rivers, have high contents of long-chain n-alkanes (C27 + C29 + C31) amounting up to 350–410 μg g_{TOC}^{-1}. Northward from the estuaries, the content of the long-chain n-alkanes decreases and reaches the minimal values (<150 μg g_{TOC}^{-1}) in the sediments of the St. Anna Trough.

Thus, the most important information on the genesis of the initial OM can be gained from the C17–C16 molecular markers typical of hydrobionts, the C19–C25 markers reflecting the contribution of the microbial and/or microbial-destructive component of the OM, and the C25–C31 typical of the terrigenous OM.

The main attention during the study of this region was traditionally focused on the diagenetic transformation of the OM in the sedimentary sequence, which was sampled using a heavy sampler with the loss of the water–sediment contact zone and, correspondingly, with the absence of data on the composition of the particulate OM and the processes of the OM's transformation in the boundary areas.

The content and distribution of the hydrocarbons from the particulate matter and sediments from site 5010 are typical of the southern termination of the profile listed in Table 14. The relative content of the n-alkane C16 (59–69 wt %) in the entire water column exceeds the total content of all the other n-alkanes (Fig. 12a). Only the suprabottom layer shows the significant enrichment of the alkanes in the long-chain component (∑C23–C35—60 wt %). The less expressed enrichment of the alkanes in the particulate matter by hexadecane was previously noted in the White Sea [13]. The production of hexadecane in marine ecosystems is also atypical, has been previously observed in some types of Antarctic krill [35], and can be explained by the specific decarboxylation of fatty acids [36].

All the studied sequences of the bottom sediments are characterized by the predominance of the high-molecular odd alkanes of the terrigenous OM (∑C23–C35, 63–91 wt %) with the maximum at C27

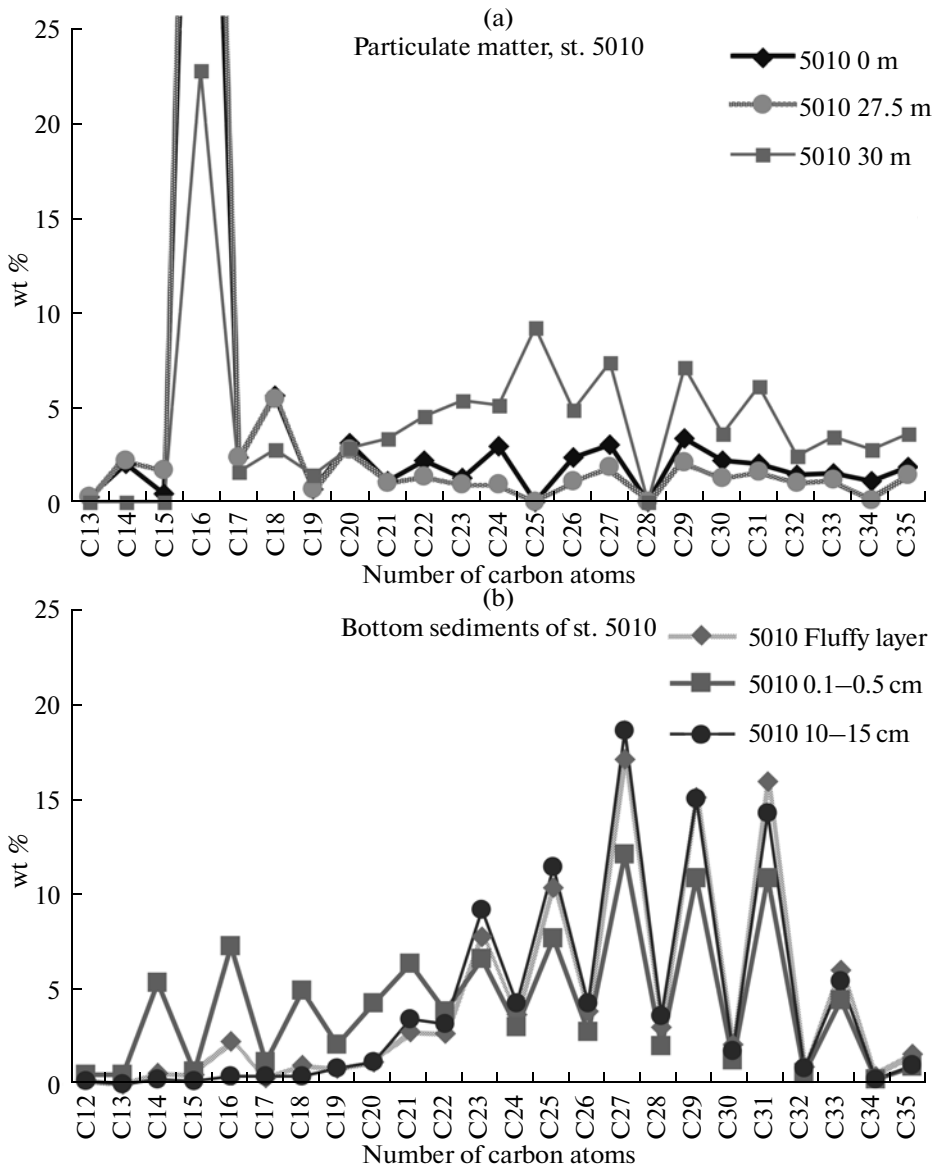

Fig. 12. Distribution of the n-alkanes in the sediments from site 5010: (a) in the particulate matter; (b) in the bottom sediments.

(Fig. 12b). However, the consideration of the low-molecular region revealed that the 0.1–0.5 horizons and, to a lesser extent, the 0.5–1 cm horizons contain even low-molecular alkanes C14–C20 (the ∑C13–C22 in the 0.1–0.5 horizon is 36 wt %). The predominance of even alkanes in the low-molecular region is rare [29], and, for the upper layer of the sediment, it can be explained only by the input of bacterial production [30].

The composition of the alkanes in the particulates principally differs from that of the bottom sediments (Fig. 12).

3. The Bottom–Pore Water's Transformation at the Water–Sediment Boundary

The hydrogeochemical analyses of the suprabottom (15–20 cm from the bottom) and the pore waters

Fig. 13. Distribution of the hydrochemical characteristics in the near-bottom water and in the pore waters of the upper sediment layer: (a) the river beds, the estuary, and the inner shelf; (b) the St. Anna Trough: (*1*) pH (NBS units); (*2*) Alk (mg equiv. L^{-1}); (*3*) PO_4 (μg-at L^{-1}); (*4*) Si (μg-at L^{-1}); (*5*) dissolved O_2 (mL L^{-1}).

(a)

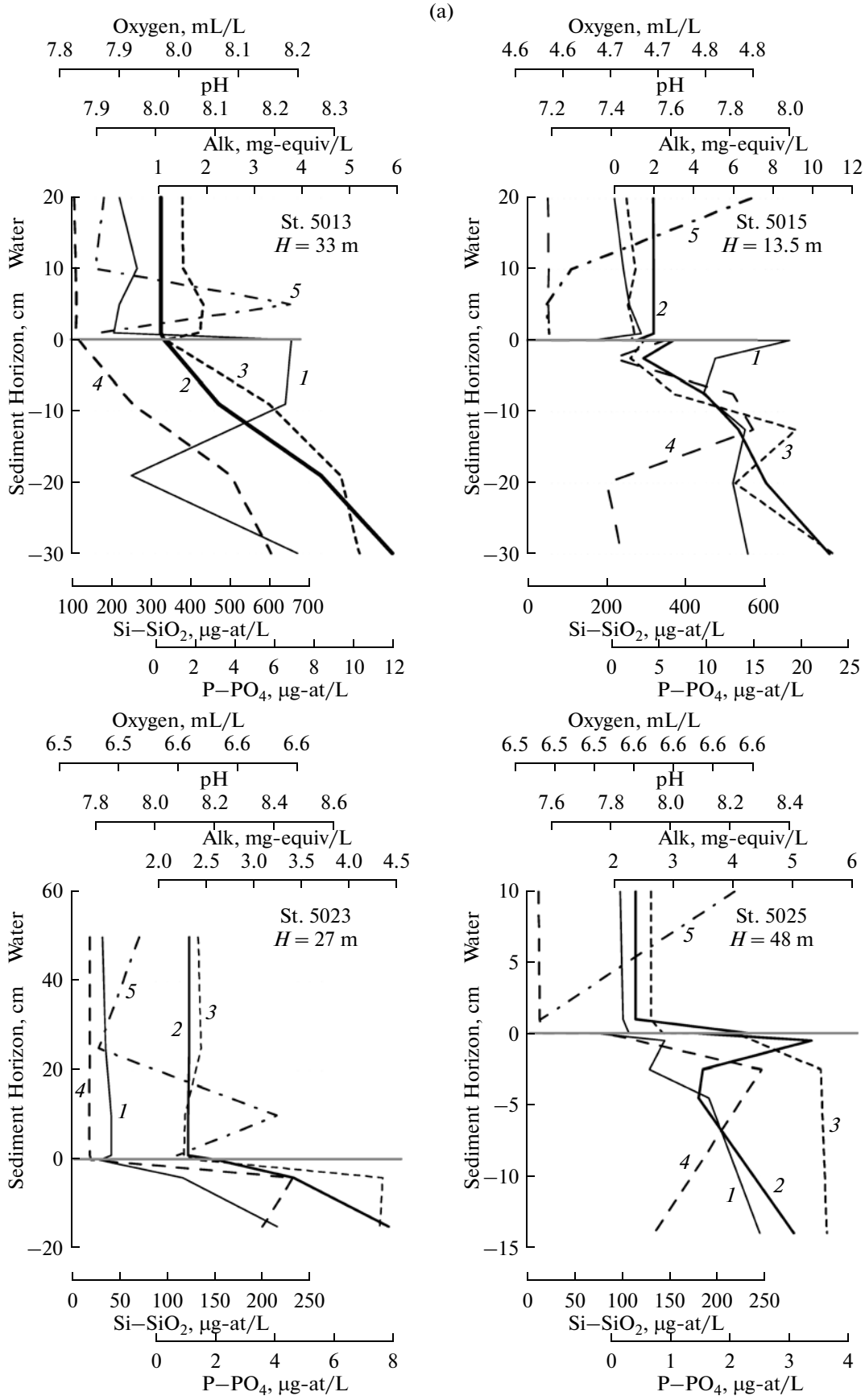
Oxygen, mL/L
pH
Alk, mg-equiv/L
St. 5013
H = 33 m
St. 5015
H = 13.5 m
St. 5023
H = 27 m
St. 5025
H = 48 m
Water
Sediment Horizon, cm
Si–SiO2, μg-at/L
P–PO4, μg-at/L

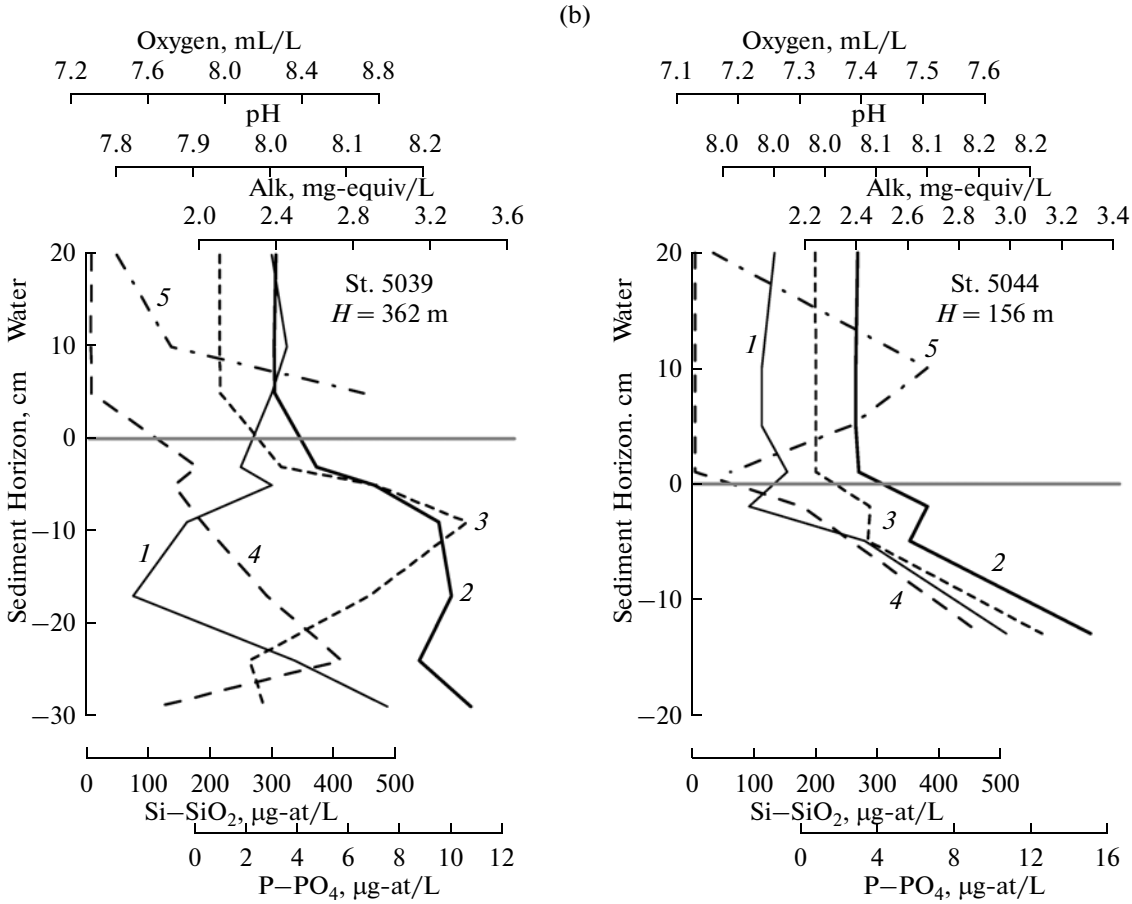

Fig. 13. (Contd.)

from the fluffy layer and the sediments were conducted for the first type at several sites of the meridional profile (Table 15, Fig. 13).

The majority of the sites show a decrease in the oxygen content from the surface water layer to the bottom.

The temperature of the suprabottom waters in September of 2011 varied from 9.59 to −1.56°C, which is close to the temperature of the bottom waters in August–September of 1993 (from 9.0 to −1.3°C) [15].

The salinity of the suprabottom waters varied in a broad range from 0.07‰ in the Yenisei River's bed to 34.95‰ in the open sea (Table 13). The contents of the sulfate and chlorine ions in the suprabottom water varied, respectively, within 0.64–28.7 mM and 0.56–545 mM (Table 14) in the river–sea direction from the south northward.

The Ca^{2+} content in the suprabottom water is the lowest at the shallow-water river sites and also increases from the south northward from 0.56 to 10.44 mM (Table 15); i.e., it reaches values typical of normal seawaters.

The hydrochemical parameters were measured in detail for the suprabottom water from the multicorer pipes and the pore water from the fluffy layer (0.0–0.5 cm) and the surface sediment layer (0.5–2.5 cm) at two sites: site 5015 (shallow-water river) and site 5025 (inner shelf) (Table 15, Fig. 13).

The fluffy layer. The fluffy layer from site 50515 has a higher pH (8) than in the suprabottom water (7.33) and the underlying sediment (7.74) (Table 15, Fig. 13). As compared to the suprabottom water and the underlying sediment, the pore water from the fluffy layer also demonstrates an increase in the total alkalinity; the dissolved phosphorus; and, especially, the silica and total nitrogen (Fig. 13). A similar pattern is observed at site 5025: the fluffy layer reveals the growth of all the biogenic elements as compared to the suprabottom water and the underlying sediment horizon (0.5–2.5 cm) (Table 15, Fig. 13).

The content of the sulfate ion in the fluffy layer from site 5025 is 0.8 mM higher than that in the suprabottom water and 0.4 mM higher than in the

Table 13. The content (%) and isotopic composition (‰) in the particulates, fluffy layer, and surface sediment horizon

Sites / Parameters	5013	5014	5015	5011-2	5010	5018	5023	5025	5026	5032	5034	5039	5042	5044	5045	5008	5007
Salinity, PSU Surface layer Near-bottom layer	 0.07 0.07	 0.06 0.07	 0.52 22.07	 13.60 32.30	 26.26 32.14	 13.91 30.97	 16.62 32.09	 22.95 33.52	 24.20 34.00	 28.64 34.05	 31.24 34.89	 31.70 34.95	 32.01 34.95	 30.89 34.80	 33.40 34.95	 14.59 30.20	 27.31 34.58
Particulated C_{org}, %, surface layer	n.a.	7.8	4.6	8.2	n.a.	1.8	1.5	7.8	1.0	n.a.	11.4	14.0	22.5	16.0	27.7	n.a.	n.a.
$\delta^{13}C$–C_{org} of the particulate matter, ‰, the surface layer	−29.73	−28.14	−30.05	−28.46	−25.11	−27.58	−26.65	−23.70	−25.39	−24.73	−23.85	−23.58	−24.01	−25.01	−24.19	n.a.	−26.98
particulated C_{org}, %, the near-bottom layer	n.a.	n.a.	3.5	13.2	n.a.	2.5	1.1	2.9	n.a.	n.a.	1.2	3.3	1.4	n.a.	3.3	n.a.	n.a.
$\delta^{13}C$–C_{org} of the particulate matter, ‰, the near-bottom layer	−29.90	−28.60	−27.55	−24.26	−25.06	−26.81	−24.00	−23.97	−23.58	−25.61	−22.84	−23.29	−23.36	−23.35	−23.02	n.a.	−22.25
the particulated C_{org}, %, the suprabottom layer	n.a.	n.a.	3.4	0.04	n.a.	1.7	n.a.	0.1	0.1	0.1	1.3	0.6	n.a.	0.2	0.2	n.a.	n.a.
the particulated $\delta^{13}C_{org}$, ‰, the suprabottom layer	−28.16	−27.72	−25.99	−25.22	−25.20	−26.13	−24.08	−23.93	−22.79	−23.47	−21.64	−20.85	−20.53	−20.95	−20.48	−26.01	−23.34
C_{org} in the fluffy layer, %	0.733	1.07	2.80	1.548	1.69	2.28	0.3232	0.6066	0.9435	0.54	1.428	1.994	1.39	0.9059	1.92	1.73	n.a.
C_{org} in the sediment, %	0.623	0.34	2.55	1.515	2.03 1.49	2.404	0.1665	0.403	0.347	0.335	1.3116	1.812	1.607	0.826	1.36	1.14	n.a.
$\delta^{13}C_{org}$ in the fluffy layer, ‰	−25.88	−26.74	−26.43	−24.62	−24.26	−25.55	−24.75	−23.01	−21.95	−23.21	−22.50	−20.82	−20.51	−20.58	−20.32	−25.08	n.a.
$\delta^{13}C$–C_{org} of the sediment, ‰	−26.02	−25.57	−26.07	−25.12	−24.53	−25.08	−23.04	−22.36	−23.06	−22.73	−22.15	−21.03	−21.02	n.a.	n.a.	−25.99	n.a.
DOC, mg L^{-1}, the suprabottom layer	6.88	8.06	4.78	1.57	1.88	2.26	1.69	1.54	1.40	4.58	3.83	1.37	0.89	2.28	1.12	5.81	12.03

Table 14. Distribution and composition (%) of the molecular markers

Site no. 5010\Molecular markers	Sediments, layer (cm)								
	Fluffy layer	0.1–0.5	0.5–1	2–5	5–10	10–15	15–20	20–25	25–33
C12	0.26	0.50	0.31	0.00	0.00	0.13	0.10	0.17	0.04
C13	0.00	0.46	0.11	0.00	0.00	0.04	0.02	0.13	0.00
C14	0.60	5.36	1.35	0.78	0.51	0.29	0.35	2.28	0.34
C15	0.53	0.69	0.70	0.14	0.10	0.19	0.12	0.25	0.08
C16	2.23	7.25	2.36	2.05	0.61	0.38	0.34	2.35	0.55
C17	0.33	1.15	0.67	0.34	0.44	0.39	0.36	0.47	0.26
C18	0.97	4.90	1.79	1.20	0.57	0.42	0.50	1.78	0.49
C19	0.79	2.09	1.80	0.82	0.84	0.80	0.69	0.97	0.70
C20	1.16	4.28	3.13	1.60	1.06	1.14	0.81	1.68	0.99
C21	2.79	6.29	3.50	2.64	3.08	3.40	2.14	3.33	3.01
C22	2.64	3.82	3.85	3.16	2.82	3.15	2.28	2.84	2.87
C23	7.74	6.60	5.71	7.23	8.47	9.20	6.23	7.34	8.33
C24	3.66	3.01	4.01	3.86	4.00	4.28	1.89	3.65	4.00
C25	10.31	7.65	7.04	10.41	10.71	11.38	7.60	9.98	11.05
C26	3.82	2.79	3.41	4.66	3.94	4.26	2.30	3.76	4.12
C27	17.07	12.10	14.65	17.25	17.64	18.56	18.19	16.53	18.05
C28	3.01	1.99	10.13	3.93	3.33	3.58	3.49	3.19	3.70
C29	15.10	10.85	11.97	14.20	15.79	14.97	18.46	14.54	15.90
C30	2.04	1.27	2.38	2.70	2.30	1.77	3.18	1.84	1.39
C31	15.94	10.85	11.67	14.46	16.00	14.22	20.06	15.19	16.43
C32	0.95	0.58	1.43	1.17	0.79	0.82	1.63	0.76	0.77
C33	6.02	4.38	4.92	5.95	5.92	5.39	7.99	5.81	5.85
C34	0.44	0.23	1.74	0.56	0.17	0.24	0.06	0.26	0.16
C35	1.60	0.93	1.37	0.90	0.92	1.02	1.22	0.90	0.90
Σ	100	100	100	100	100	100	100	100	100
Site no. 5010	Fluffy layer	0.1–0.5	0.5–1	2–5	5–10	10–15	15–20	20–25	25–33
C_{org}, %	1.69	2.08	1.49	1.57	1.81	0.88	1.09	1.39	1.53
n-alk., μg/g	5.07	7.81	3.12	4.81	4.29	1.96	1.56	4.46	4.01
i-C19/*i*-C20	7.81	2.40	1.92	1.88	2.67	4.47	0.06	1.22	2.30
i-C19/C17	3.11	0.98	1.12	0.51	0.70	0.76	0.00	0.38	0.54
i-C20/C18	0.13	0.09	0.22	0.08	0.20	0.16	0.00	0.08	0.12
ΣEven	21.78	35.98	35.90	25.66	20.10	20.45	16.93	24.57	19.42
ΣOdd	78.22	64.02	64.10	74.34	79.90	79.55	83.07	75.43	80.58
CPI	3.59	1.78	1.79	2.90	3.98	3.89	4.91	3.07	4.15
ΣC13+C22/ΣC23+C35	0.14	0.57	0.24	0.15	0.11	0.11	0.08	0.19	0.10
ΣC13-C22	12.0	36.3	19.3	12.7	10.0	10.2	7.6	16.1	9.3
ΣC18-C22	8.4	21.4	14.1	9.4	8.4	8.9	6.4	10.6	8.1
ΣC20-C24	18.0	24.0	20.2	18.5	19.4	21.2	13.4	18.8	19.2
ΣC23-C35	87.7	63.2	80.4	87.3	90.0	89.7	92.3	83.8	90.7
n-alk., μg/g	5.07	7.81	3.12	4.81	4.29	1.96	1.56	4.46	4.01

Table 14. (Contd.)

Site no. 5010	Particulate matter , layer				
	0 m	5 m	20 m	27.5 m	30 m
C13	0.24	n.a.	0.19	0.22	n.a.
C14	2.00	1.16	3.23	2.18	n.a.
C15	0.42	1.57	1.68	1.67	n.a.
C16	59.43	67.21	67.74	69.15	22.73
C17	2.38	2.49	2.11	2.30	1.57
C18	5.64	5.38	4.76	5.45	2.78
C19	0.68	0.80	0.61	0.65	1.41
C20	3.07	2.83	2.29	2.74	2.88
C21	1.07	1.22	0.89	0.99	3.35
C22	2.20	1.91	1.65	1.36	4.51
C23	1.27	1.19	1.06	0.94	5.34
C24	2.95	1.04	1.27	0.94	5.11
C25	n.a.	n.a.	n.a.	n.a.	9.23
C26	2.34	1.24	1.62	1.05	4.81
C27	2.98	2.23	1.99	1.81	7.33
C28	n.a.	1.56	n.a.	n.a.	n.a.
C29	3.31	1.99	2.32	2.06	7.09
C30	2.18	1.19	1.45	1.28	3.61
C31	2.02	1.39	1.52	1.56	6.11
C32	1.45	0.93	1.07	1.03	2.41
C33	1.50	1.01	1.00	1.14	3.40
C34	1.09	0.11	0.03	0.06	2.73
C35	1.81	1.54	1.52	1.41	3.58
Σ	100	100	100	100	100
Site no. 5010	0 m	5 m	20 m	27.5 m	30 m
C_{org}, μg/L^{-1}	152.19	95.8	81.75	149	2538
n-alk., ng/L	626	137	207	279	235
i-C19/*i*-C20	3.07	4.83	7.14	5.02	1.86
i-C19/C17	1.17	2.14	1.91	1.91	1.34
i-C20/C18	0.16	0.20	0.12	0.16	0.41
ΣEven	82.34	84.56	85.10	85.23	51.59
ΣOdd	17.66	15.44	14.90	14.77	48.41
CPI	0.21	0.18	0.18	0.17	0.94
ΣC13+C22/ΣC23+C35	3.37	5.48	5.73	6.52	0.65
ΣC13-C22	77.1	84.6	85.1	86.7	39.2
ΣC18-C22	12.7	12.1	10.2	11.2	14.9
ΣC20-C24	10.6	8.2	7.2	7.0	21.2
ΣC23-C35	22.9	15.4	14.9	13.3	60.8
n-alk., ng/L	626.49	136.81	207.46	279.37	235.45

pore water from the horizon of 0.5–2.5 cm (Table 15). In our opinion, this difference is related to the influx of reduced and semioxidized sulfur compounds from the sediments into the fluffy layer and their transformation into sulfate ions at the contact with the water column.

Thus, the fluffy layer demonstrates the peak of the dissolved biogenic elements and the sulfate ions as compared to the suprabottom water and surface sediment horizon (Table 15, Fig. 13).

The sediments (the horizon of 0.5–2.5 cm). The pore water from the sedimentary sequence shows an increase in the content of the biogenic elements, the decomposition products of the OM, and a decrease in the sulfate ion from the top to the bottom. Similar tendencies are observed at all the transitional sites

Table 15. Hydrogeochemical parameters and salt composition of the pore waters in the sediments along the meridional profile of the Yenisei River–St. Anna Trough in the Kara Sea

Horizon, cm	C_{org}, %	pH	SO_4^{2-}, mM	Cl^-, mM	Alk, mg-equiv. L^{-1}	Ca^{2+}, mM	Mg^{2+}, mM	PO_4, μg-at. L^{-1}	Si, μg-at. L^{-1}	N_{tot}, μg-at. L^{-1}
St. 5007										
Suprabottom water	–	7.72	28.9	542	2.505	10.44	56.46	2.48	42.23	28.10
1–2	1.416	7.92	30.4	569	2.906	11.80	56.90	9.81	457.39	290.37
2–5	1.712	8.04	29.3	565	3.407	11.72	56.28	14.00	441.26	302.49
5–17	1.733–1.743	8.19	29.3	550	3.407	10.65	53.06	25.91	225.85	437.95
17–40	1.367–1.596	8.21	29.7	550	3.607	10.37	52.44	14.0	166.54	608.61
St. 5008										
2–7	1.31	7.72	27.2	512	2.605	10.01	49.21	3.72	258.59	193.48
7–17	1.176	7.94	28.4	525	2.405	9.72	48.40	2.19	185.04	274.24
St. 5010										
Suprabottom water	–	–	26.9	518	–	–	–	–	–	–
2–9	1.69	8.14	27.6	532	3.407	9.77	49.45	0.95	232.96	488.95
9–16	1.57–1.81	8.06	26.5	520	3.657	9.30	47.53	7.14	294.65	316.77
16–30	1.09–1.53	8.24	26.1	523	4.208	9.17	46.86	6.29	206.87	319.02
St. 5013										
Suprabottom water	–	8.23	0.64	0.56	1.102	0.56	0.27	0.48	116.25	109.49
5–9	0.438	8.22	2.57	52	2.255	1.00	2.78	5.72	252.42	554.94
9–19	1.160	7.96	10.7	197	4.409	4.09	18.94	9.34	501.04	513.28
19–30	0.240	8.24	15.6	304	5.912	6.89	29.20	10.29	603.05	542.16
St. 5014										
Fluffy layer	1.07	–	0.86	–	–	–	–	–	–	–
Suprabottom water	–	_	0.43	0.56	–	0.44	0.40	–	119.57	42.53
0.5–1.5	0.34–0.49	–	0.86	–	–	–	–	–	–	
1.5–17	0.48	8.27	2.57	7.6	1.202	0.41	0.84	84.59	269.50	801.68
St. 5015										
Suprabottom water	–	7.33	18.4	348	1.052	6.88	36.09	2.00	58.36	86.52
Fluffy layer	2.80	8.00	–	–	2.906	–	–	3.33	344.94	188.98
0.5–2.5	2.55	7.75	19.7	428	1.403	–	–	1.91	213.04	50.99
2.5–7.5	1.25–2.33	7.71	18.2	366	4.509	7.62	35.06	6.57	516.70	445.82
7.5–12.5	2.11	7.85	16.0	347	6.212	6.99	32.79	19.34	566.99	598.36
12.5–20	2.27	7.81	15.6	349	7.615	6.72	32.16	12.96	197.85	–
20–30	2.43	7.86	12.8	360	10.822	6.13	33.35	23.34	235.34	–
St. 5018										
0.5–5.0	2.404	–	26.3	502	–	9.56	48.46	15.81	154.68	–
5–10	2.270	7.91	26.3	512	3.908	9.84	47.19	14.96	141.87	–
10–15	2.379	7.93	25.2	516	4.359	9.85	48.18	9.91	139.49	–
15–20	2.010	8.01	25.7	588	5.110	–	–	–	302.71	–

Table 15. (Contd.)

Horizon, cm	C_{org}, %	pH	SO_4^{2-}, mM	Cl^-, mM	Alk, mg-equiv. L^{-1}	Ca^{2+}, mM	Mg^{2+}, mM	PO_4, μg-at. L^{-1}	Si, μg-at. L^{-1}	N_{tot}, μg-at. L^{-1}
St. 5011-2										
Suprabottom water	–	7.80	24.2	484	2.204	9.37	50.45	1.62	23.25	47.82
5–10	1.318	–	25.4	580	2.488	–	–	–	–	574.94
10–14	0.940	–	22.2	–	2.14	–	–	–	–	783.11
14–24	1.160	8.40	19.7	536	13.427	8.28	46.86	–	–	911.90
24–30	1.010	8.39	19.0	556	12.525	–	–	32.96	302.71	981.51
St. 5023										
Suprabottom water		7.81	26.3	512	2.605	9.91	53.70	–	–	–
0–1	0.166	–	27.2	526	–	10.35	51.46	1.33	18.98	53.38
1–4	0.249	8.09	27.2	522	3.407	9.97	49.25	–	–	330.99
4–15	0.6315	8.41	25.9	522	4.409	9.02	46.91	7.62	232.02	487.04
St. 5025										
Suprabottom water	–	7.86	27.8	534	4.275	10.42	56.18	0.86	15.66	29.74
Fluffy layer	0.944	7.75	28.6	567	3.407	–	–	2.10	82.08	85.15
0.5–2.5	0.846	7.93	28.2	550	3.474	10.57	55.03	3.52	245.78	165.50
2.5–4.5	0.650	8.13	28.6	650	3.407	–	–	–	–	247.86
4.5–14.0	0.695	–	–	–	–	–	–	3.62	132.85	298.03
St. 5026										
Suprabottom water	–	7.98	28.7	539	2.405	10.44	55.46	0.95	16.13	242.25
0.5–2.5	0.846	7.95	28.2	550	2.872	10.72	54.39	–	–	305.81
2.5–8.0	0.650	–	28.7	596	–	–	–	3.43	242.93	496.95
8.0–13.5	0.695		29.9							459.28
St. 5032										
Suprabottom water	–	–	28.1	545	–	–	–	–	–	–
0–2	0.430	–	28.9	549	–	10.59	53.72	–	–	–
2–5	0.379	–	28.6	577	–	11.36	56.93	–	–	–
5–12	0.160	–	27.2	551	–	10.65	51.98	–	–	–
12–20	0.440	–	23.6	–	–	–	–	–	–	–
St. 5033										
Fluffy layer	0.860	7.90	27.8	540	2.405	10.76	56.24	1.62	83.51	45.48
0–1	0.826	7.67	31.7	550	2.739	10.76	53.75	2.86	222.53	263.37
1–3	0.809	7.80	29.8	582	2.305	–	–	2.48	228.22	80.38
3–6	0.683–0.750	8.01	29.1	573	2.872	11.14	56.34	4.10	230.59	258.68
6–16	0.485–0.530	8.47	29.6	571	3.507	10.32	53.20	3.33	133.80	508.63
16–24	0.559–0.700	8.33	29.3	562	4.108	10.22	53.30	2.38	173.66	381.42
St. 5034										
Fluffy layer	1.428	7.99	27.8	528	2.405	10.02	54.78	1.33	27.52	29.85
0–1	1.312	7.68	29.9	567	3.273	11.44	57.54	2.10	190.74	102.33
1–3	1.628	7.95	29.9	578	3.073	11.80	58.57	2.48	199.28	124.02
3–13	0.950–1.240	–	29.9	562	–	10.65	53.76	–	–	–
13–23	0.770	–	30.6	570	–	10.60	53.42	–	–	–
23–30	0.740	8.28	32.9	–	4.309	–	–	1.71	113.40	542.18

Table 15. (Contd.)

Horizon, cm	C_{org}, %	pH	SO_4^{2-}, mM	Cl^-, mM	Alk, mg-equiv. L^{-1}	Ca^{2+}, mM	Mg^{2+}, mM	PO_4, μg-at. L^{-1}	Si, μg-at. L^{-1}	N_{tot}, μg-at. L^{-1}
St. 5039										
1–3	1.812	7.96	31.0	584	2.6i05	11.62	–	3.33	178.88	170.56
3–5	1.510	8.00	34.6	–	2.906	–	–	7.05	140.44	409.69
5–9	0.930	7.89	30.8	592	3.240	12.46	59.40	10.57	186.47	348.32
9–17	1.070	7.82	29.7	557	3.307	10.76	54.64	6.76	292.27	314.11
17–24	1.250	8.03	29.7	594	3.140	12.44	–	2.10	413.74	377.64
24–29	1.030	8.15	–	–	3.407	–	–	2.67	115.30	464.95
St. 5042										
0–2	1.607	7.73	30.8	559	2.472	11.02	55.28	2.76	226.32	164.87
2–4.5	1.413	7.82	29.3	598	2.572	11.66	–	3.91	207.82	161.65
4.5–7.5	1.489	7.86	33.4	–	2.739	–	–	6.48	179.82	360.93
7.5–14.5	1.692	–	–	–	–	–	–	3.33	123.84	594.10
14.5–17.0	1.511	–	–	–	–	–	–	1.71	405.67	490.51
17.0–27.0	1.550	7.71	29.6	577	3.206	11.20	52.68	2.38	199.28	378.26
St. 5044										
0–2	0.826	7.98	30.0	584	2.672	13.13	–	3.55	177.45	218.88
2–5	0.859	8.07	32.1	630	2.605	–	–	3.45	256.69	163.04
5–13	0.530	8.18	30.0	587	3.307	12.11	59.05	2.86	506.26	291.24
St. 5045										
0–1.5	2.25	8.01	30.2	–	2.806	–	–	1.92	224.42	275.73
1.5–3.5	2.02	8.08	32.1	–	2.705	–	–	3.45	267.13	464.04
3.5–13.5	2.00	8.23	26.3	578	2.939	11.86	65.76	1.53	116.25	187.56
13.5–25	1.86	–	29.6	563	–	10.52	64.71	–	–	–
25–35	1.95	8.22	30.4	619	3.006	12.34	63.28	1.43	460.24	562.67

Note: Denotes that determinations are absent.

between the two terminal sites (sites 5015 and 5025) along the meridional profile.

The characteristics of the pore waters obtained for the Yenisei River–Sea meridional profile in September of 2011 slightly differ from the composition of the pore waters measured in August–September of 1993 [15]. The changes in their composition along the vertical sections of the sediments are different in the south and north of the profile, which is primarily determined by the rate of the early diagenetic processes.

This difference in the concentrations generates diffusion fluxes of chemical components via the water–bottom boundary. We attempted to estimate these fluxes on the basis of the concentration gradients between the suprabottom water and the pore water for the sites of the Yenisei section in the area where we managed to sample the fluffy layer (sites 5015 and 5025, Table 16). The higher concentrations of chemical components in the pore water as compared to the suprabottom water define the predominant direction of the diffusion fluxes from the sediments, although, in some cases, they could have an opposite direction.

Table 16. The Yenisei section: the fluxes of dissolved chemical components at the water–bottom boundary (the calculations were performed by A.G. Rozanov for the 0.3-cm fluffy layer and the 3-cm bottom sediment)

Components	Cl^-	SO_4^{2-}	Alk	Ca^{2+}	Mg^{2+}	HPO_4^{2-}	H_4SiO_4
	mM m^{-2} day^{-1}					μM m^{-2} day^{-1}	
Site 5015 (estuary, depth 7.8 m)							
Fluffy layer	n.a.	n.a.	19.1	n.a.	n.a.	7.10	2820
Bottom sediment	157	1.28	0.36	0.55	–0.71	–0.05	152
Site 5025 (inner shelf, depth 48 m)							
Fluffy layer	646	8.04	–8.95	n.a.	n.a.	6.57	6.54
Bottom sediment	31.3	0.39	–0.83	0.11	–0.86	1.43	226

Note: 1. The calculations were performed using the formula of Fick's first law: $J = -D^0 dC/dx$, where the flux of the dissolved component (J) is proportional to the gradient (dC/dx) of the concentration (C) over the layer's thickness x. The thickness of the fluffy later was taken to be 0.3 cm, and the thickness of the upper layer of the sediment is 3 cm. The molecular diffusivity (D^0) in seawater for each component at the selected temperature, as the details of the calculations for the bottom sediments, was taken from [22, 23, 28, 37]. 2. The minus sign denotes that the diffusion flux is directed against the gradient, i.e., from the higher to lower concentrations. In this case, an increase of the concentrations in the sediment with the depth gives negative gradients and positive values of the fluxes directed upsection, and vice versa.

The concentrations in the fluffy layer are always higher than those in the sediments, and, correspondingly, the fluxes from the fluffy layer (0.3 cm) are usually much higher than those from the sediment (3 cm). An exception is the dissolved silica, whose concentrations in the fluffy layer are lower than in the pore water of the sediments from the inner shelf (site 5025, depth 48 m), and, correspondingly, the flows from the sediments into the suprabottom water are higher than those from the fluffy layer. In contrast, the fluffy layer of the estuary (site 5015, depth 7.8 m) has an extremely high content of silica, which is capable of providing a much higher flux than that from the sediments. The Mg fluxes are always directed to the sediment, while the Ca fluxes usually move from the sediments. The flows of CO_2 (Alk) usually directed from the sediment into the suprabottom water at the inner shelf (site 5025) may change their direction. Note that the diffusion fluxes at the water–bottom boundary account for only part of the chemical exchange, which also includes the mechanical exchange (the near-bottom currents, the tidal and wave phenomena especially expressed at the shoals, and the advection within the sediment) and the bios-related exchange (bioturbation, bioirrigation). The distribution of the concentrations and fluxes of the chemical elements at the water–bottom boundary and in the sedimentary sequence requires special consideration of both the physical and biogeochemical processes.

The rate of the early diagenetic reducing processes can be estimated not only from the consumption of the sulfate ion and the growth of the total alkalinity in the muds but also from the isotopic sulfur composition of the sulfate ion. The sulfates in the river waters are depleted in the ^{34}S heavy isotope ($\delta^{34}S = 18.8‰$) as compared to the marine sulfates ($\delta^{34}S = 19.6–20.5‰$), which confirms the conclusion concerning the strong influence of the fresh waters in the southeastern and eastern areas of the Kara Sea [15].

The content of the sulfur species was measured in some sedimentary samples taken in September of 2011 (Table 17). The sum of the reduced sulfur species (ΣS_{H_2S}) varies from 0.025% in the horizon of 2–5 cm on the outer shelf (site 5007) to 0.116% in the horizon of 24–30 cm in the estuary (site 5011-2).

The ΣS_{H_2S} contains monosulfide sulfur (hydrotroilite), pyrite sulfur (S_{pyr}), and organic sulfur (S_{org}). Black films of hydrotroilite were noted in the muds of all the distinguished facies (Table 17). The highest content of organic sulfur (0.048%) was found in the sediments of the estuarian facies (site 5018, Table 17).

Based on the results of the cruise of 1993, the isotopic composition of the pyrite sulfur in the surface sediment

Table 17. Content of sulfur species* in the bottom deposits of the Yenisei profile

Site no.	Horizons, cm	S_{SO_4}, %	$S_{sulfide}$, %	$S_{pyr\text{-}elem}$, %	S_{org}, %	ΣS_{H_2S}, %
5007	2–5	0.076	0.003	0.004	0.018	0.025
	5–17	0.116	0.002	0.004	0.022	0.028
	17–40	0.123	0.039	0.009	0.026	0.075
5010	2–9	0.030	0.007	0.007	0.013	0.027
	9–16	0.023	0.015	0.017	0.016	0.049
	16–30	0.062	0.043	0.026	0.034	0.102
5011-2	5–10	0.059	0.013	0.022	0.021	0.056
	10–14	0.056	0.005	0.014	0.019	0.037
	14–24	0.019	0.035	0.022	0.025	0.083
	24–30	0.012	0.035	0.058	0.023	0.116
5013	9–19	0.005	0.041	0.031	0.013	0.085
	19–30	0.002	0.008	0.017	0.008	0.032
5018	5–10	0.038	0.002	0.011	0.048	0.061
	10–15	0.046	0.002	0.011	0.025	0.038
5026	2.5–8	0.028	0.039	0.018	0.023	0.080
	8–13.5	0.029	0.026	0.017	0.013	0.057

Note: All the samples were collected using a multicorer; the determination of the different sulfur species was carried out using the technique of systematic phase analysis, which allowed for the determination of the different sulfur species from one sediment sample [4]. All the concentrations are given in the calculations for the dry residue.

The $S_{sulfide}$ is the sulfur of acid-soluble sulfides. The weighted samples of the bottom sediments of natural moisture were treated with HCl and heated to boiling with the simultaneous extraction of the released H_2S by inert gases and iodometric termination.

The $S_{pyr\text{-}elem}$ (pyrite sulfur) was determined, together with the elementary sulfur, after the reduction by a $CrCl_2$ solution to H_2S, whose amount was determined by volume iodometric titration.

The S_{org} is the sulfur bound with the organic (mainly with the humic) matter of the sediment. The sediment remaining after the extraction of the sulfide and pyrite species of sulfur was subjected to exhaustive oxidation, thus transforming the organic sulfur into sulfate, whose content was determined gravimetrically.

The S_{SO_4} is the total sulfate sulfur of the sediments. It was determined using the filtrate obtained after the determination of the sulfide sulfur and combined with the rinsing waters. The sulfates were precipitated as $BaSO_4$ and, after annealing at 800–850°C, were determined gravimetrically.

* The analyst was N.M. Kokryatskaya.

horizons (0–10 cm) varied from –8.4‰ in the estuary of the Yenisei River to –22.9 ‰ in the northern part of the sea far removed from the influence of the river waters with isotopically light sulfate ion [15].

The distribution of the concentrations and the values of $\delta^{34}S$ of the sulfate ion suggests that a biogeochemical sulfur cycle operates in the sediments with different intensity: from the consumption of the sulfate ion to the new formation of isotopically light sulfates during the oxidation of the reduced compounds supplied from the sediments.

4. The Rate of the Sulfate Reduction in the Fluffy Layer and the Surface Sediment Horizon

Sulfate reduction was found in all the studied samples of the fluffy layer and surface sediment horizons. The rate of this process varies within a broad range: from 1719.3 μgS dm^{-3} day^{-1} (site 5010, Table 18) to 9.9 μgS dm^{-3} day^{-1} (site 5026, Table 18). The fluffy layer from site 5010 has the highest content of n-alkanes of microbial genesis.

At most of the sites of the meridional profile, the rate of the sulfate reduction in the fluffy layer is lower than in the horizon of 0.5–1 cm (Table 18). Exceptions are sites 5032 and 5042–5045 (the St. Anna Trough), where the rate of the sulfate reduction in the fluffy layer is higher than in the horizon of 0.5–1 cm (Table 18). This presumably indicates that these differ from the southern sites of the meridional profile in the content and composition of the OM in the fluffy layer. At the southern sites with a sulfate reduction rate of less than 100 μgS dm^{-3} day^{-1}, the rate of the sulfate reduction increases as the C_{org} content increase (Table 18).

Table 18. Rate of the sulfate reduction (SR) in the fluffy layer and sediments along the Yenisei R.–St. Anna Trough meridional profile

Site	Horizon, cm	FeSn, μgS dm^{-3} day^{-1}	$FeS_2 + S_{org}$, μgS dm^{-3} day^{-1}	Rate $SR_{tot.}$ μgS dm^{-3} day^{-1}
5007	Fluffy layer	8.63	38.71	47.34
	0.5–5.0	4.16	42.82	46.99
5010	Fluffy layer	1018.83	3.63	1022.46
	0.5–5.0	1593.63	125.70	1719.34
5013	Fluffy layer	50.02	0.80	50.82
	0.5–1.0	77.06	19.25	96.30
	1.0–5.0	96.05	62.56	158.61
5018	Fluffy layer	56.13	11.27	67.40
	0.5–1.0	63.11	22.32	85.44
	1.0–5.0	68.26	55.60	123.86
5011"	Fluffy layer	43.97	40.48	84.45
	0.5–1.0	20.79	82.27	103.05
	1.0–5.0	17.36	18.60	35.96
5026	Fluffy layer	2.70	7.22	9.93
	0.5–1.0	1.46	17.20	18.66
5032	Fluffy layer	1.66	137.87	139.54
	0.5–1.0	1.92	79.04	80.97
	12.0–20.0	–3.07	149.88	146.81
5033	Fluffy layer	–0.36	68.60	68.23
	0.5–5.0	1.25	110.38	111.63
5039	Fluffy layer	–1.46	54.05	52.59
	0.5–5.0	3.79	120.46	124.26
5042	Fluffy layer	10.00	207.54	217.55
	0.5–5.0	6.60	199.94	206.54
	8–15	4.32	33.13	37.46
	48–53	2.23	3.67	5.90
	98–103	–1.22	2.80	1.57
	148–153	79.07	–0.70	78.37
	198–203	–1.05	37.46	36.41
	228–233	–2.27	76.34	74.07
	278–283	–3.36	7.82	4.46
5044	Fluffy layer	17.83	74.37	92.19
	0.5–5.0	11.07	52.96	64.03
5045	Fluffy layer	4.42	54.83	59.24
	0.5–5.0	–0.57	18.97	18.40

The fluffy layer from the river and estuarian sites is characterized by a sulfate reduction rate within 0.01–1.72 μgS dm^{-3} day^{-1} with an average value of 0.0245 μgS dm^{-3} day^{-1} (five samples). The fluffy layers from the marine sites of the inner and outer shelf show variations in the sulfate reduction rate within 0.047–0.139 μgS per dm^{-3} day^{-1} with an average value of 0.077 μgS dm^{-3} day^{-1} (four samples). In the fluffy layer

Table 19. Concentrations of methane and the rate of the methanogenesis (MG) in the fluffy layer and sediments along the Yenisei R.–St. Anna Trough profile

Site no.	Horizon, cm	CH_4, μM dm^{-3}	Rate of MG, nM dm^{-3} day^{-1}
The Yenisei R.: the bed, estuary, and inner shelf			
5010	fluffy layer	1.53	1.46
	0.5–5.0	2.82	1.23
		2.69	n.a.
5011-2	fluffy layer	1.28	0.90
	0.0–0.05	1.45	n.a.
	0.5–1.0	4.31	1.82
	1.0–5.0	4.11	2.70
5013	fluffy layer	0.84	1.38
	0.5–1.0	1.04	3.81
	1.0–5.0	1.20	4.52
5018	fluffy layer	1.24	tr.
	0.5–1.0	1.32	tr.
	1.0–5.0	2.08	1.02
5023	fluffy layer	0.91	n.a.
	0.0–0.5	7.79	n.a.
	0.5–2.0	6.48	n.a.
5026	fluffy layer	1.37	1.68
	0.5–1.0	2.27	2.05
	1.0–2.0	2.59	2.82
	8.0–10.0	2.04	n.a.
5008	fluffy layer	3.18	1.97
	0.0–0.5	22.71	4.10
Outer shelf–St. Anna Trough			
5032	fluffy layer	0.55	1.91
	0.5–1.0	1.62	2.92
	12.0–20.0	4.44	2.50
5033	fluffy layer	0.55	2.58
	0.5–5.0	2.15	4.83
	6.0–10.0	2.63	4.32
5039	fluffy layer	0.13	1.91
	1.0–5.0	0.32	1.82
	17.0–19.0	0.12	n.a.
5042	fluffy layer	0.01	3.58
	1.5–5.0	0.30	3.75
	2.0–4.5	0.12	4.64
	4.5–7.5	0.27	4.44
	7.5–14.5	0.25	n.a.
	14.5–17.0	0.49	n.a.
	17.0–27.0	0.11	n.a.
5044	fluffy layer	0.02	5.31
	1.5–5.0	0.69	11.66
	5.0–8.0	0.85	n.a.
5045	fluffy layer	0.03	5.50
	0.5–5.0	n.a.	10.12
Outer shelf			
5007	fluffy layer	2.38	tr.
	0.5–2.0	4.89	tr.
	2.0–5.0	4.39	n.a.
	5.0–17.0	5.12	n.a.

Note: n.a. means not analyzed; tr. means traces.

from the sediments of the St. Anna Trough, the rate of the sulfate reduction varies from 0.218 to 0.059 μgS dm^{-3} day^{-1}, while averaging 0.123 μgS dm^{-3} day^{-1} (three samples). Such a distribution of the sulfate reduction rate is consistent with the distribution of the Eh value.

In the surface layer of the muds, the values of the sulfate reduction rate at most of the sites are higher than in the fluffy layer, although they also lie within the interval of 0.076–0.096 μgS dm^{-3} day^{-1} obtained during the cruise in the Kara Sea in the autumn of 1993 [15].

The average rate of the sulfate reduction in the fluffy layer and the surface sediment horizons along the meridional profile in the Kara Sea is comparable with that in the shallow-water sediments of the Northern Sea and the Californian Bay [40].

The rate of the sulfate reduction in the fluffy layer and the sediment indicates the activity of the heterotrophic and autotrophic sulfate reducing microorganisms not only under reducing but also under reducing–oxidizing conditions at the contact with the water column containing from 5.64 to 7.45–8.72 mL L^{-1} oxygen. The process proceeds within aggregates, where "niches" with reducing conditions are created.

As reported previously, the production of reduced sulfur in the Kara Sea is 24×10^6 t per year, and only 2% are buried in the sediments [15]. There are no grounds to revise this value, because the rates of the sulfate reduction in the surface deposits obtained during the cruise in 2011 are similar to those measured in 1993 [15].

The similarity of the sulfate reduction rate in the fluffy layer and the horizon of 0.5–1 cm emphasizes the high intensity of the exchange processes in the sulfur cycle at the fluffy layer–sediment contact.

5. The Methane Concentration and the Rate of the Methane Genesis in the Fluffy Layer and in the Surface Sediments

The concentration of methane in the fluffy layer varies within 0.84–3.18 μM dm^{-3} at the southern sites affected by the fresh waters. At the marine sites on the inner and outer shelf, the methane concentration in the fluffy layer varies from 0.55 to 2.38 μM dm^{-3}, while the fluffy layer from the deep-water sites of the St. Anna Trough has the lowest CH_4 content of 0.01–0.13 μM dm^{-3} (Table 19).

In the surface sediment horizon of 0.5–2 cm, the content of methane is approximately 1.5–7 times higher than in the fluffy layer. Methane is supplied in the fluffy layer and the water column from the sediments generating it. Experiments on the rate of the methane genesis from CO_2 showed that the microbial formation of methane from CO_2 in the fluffy layer and surface sediment horizons is very weak, being close to the background values. Only at sites 5044 and 5045 in

Table 20. Content and isotopic composition of the carbonates in the fluffy layer and sediments from the meridional profile

Site no.	Horizon, cm	C_{carb}, %	Carbonate minerals, %	$\delta^{13}C$, ‰
5013	0.0–1.0	0.18	1.52	–4.62
	1.0–5.0	0.074	0.62	
	5–9	n.a.	n.a.	–3.56
	9–19	n.a.	n.a.	–3.71
	19–30	n.a.	n.a.	–6.49
5014	fluffy layer	0.259	2.19	n.a.
	0.0–0.5	0.291	2.46	n.a.
5015	fluffy layer	0.697	5.88	n.a.
5018	fluffy layer	1.02	8.61	n.a.
	0.0–0.5	0.491	1.61	n.a.
5025	fluffy layer	0.118	0.996	n.a.
	0.0–0.5	0.142	1.20	n.a.
5026	fluffy layer	0.124	1.05	n.a.
	0.0–0.5	0.282	2.38	–3.5
5010	0.0–0.5	0.207	1.75	n.a.
	0.5–2.0	0.401	3.38	n.a.
5011-2	1.0–5.0	n.a.	n.a.	–4.45
	5.0–10.0	n.a.	n.a.	–3.54
	10.0–14.0	n.a.	n.a.	–1.99
	24.0–30.0	n.a.	n.a.	–7.53
5032	0–2	n.a.	n.a.	–6.03

Note: n.a. means not analyzed; tr. means traces.

the St. Anna Trough does the value of the methane genesis in the reduced sediments reach 10–12 nM of CH_4 dm^{-3} day^{-1} (Table 19), which exceeds the background values.

Under less reducing conditions, methane oxidation prevails in the fluffy layer, while the fluffy layer itself generates less methane than the underlying horizon of the surface sediments.

The obtained values of the methane concentration are close to the previously known data, which makes it possible to use the value of 15–17 mL of CH_4 m^{-2} day^{-1} calculated for the methane flux in the atmosphere from the bottom deposits of the Yenisei River estuary from the data of 1993 [16].

Studies carried out for many years by the researchers of the Vernadsky Institute of Geochemistry and Analytical Chemistry of the Russian Academy of Sciences [5] showed that the values of $\delta^{13}C$-CH_4 in the sediments from the southeastern part of the Kara Sea are depleted in the ^{13}C heavy isotope ($\delta^{13}C$-CH_4 is up to –100‰), which unambiguously confirms the microbial (diagenetic) genesis of methane in the Holocene muds of the studied area.

6. The content of Carbonates in the Fluffy Layer and in the Sediments of the Yenisei River's Bed, the Estuary, and the Inner Shelf

At the shallow-water river sites 5014 and 5018, the content of carbonate minerals in the fluffy layer varies from 2.19 to 8.61% (Table 20). All these minerals are terrigenous in origin. The content of carbonate minerals in the fluffy layer of the deep-water estuarian sites

Fig. 14. Carbonate nodule on the surface of the sediment from site 5302.

(sites 5025 and 5020) decreases to 0.996–1.05% (Table 20). The values of $\delta^{13}C\text{-}C_{carb}$ vary from –3.50 to 6.03‰. It is suggested that the carbonate minerals are transported from the water drainage area and preserved mainly in the particulate matter and fluffy layer. In the aggressive environment of the subsurface horizons with an elevated HCO_3^- content, they gradually dissolve instead of being buried, thus providing for the almost complete absence of the carbonate component in the sediments.

The authigenic isotopically light carbonates that are formed during methane oxidation in the deposits of the Kara Sea [5, 16] were not found during the cruise of 2011. Nodules (Fig. 14) with an isotopic composition from –14.00 to –24.00‰ were formed with the participation of the isotopically light carbon of the organic matter of the sediments; i.e., they are authigenic in origin.

CONCLUSIONS

The complex studies of the water column, fluffy layer, and surface sediments carried out in September of 2011 with an emphasis on the contact zone between the water column and the bottom deposits allowed the following conclusions to be reached:

(1) The fluffy layer from 1 mm to 0.5 and more cm thick usually exists at the water–bottom boundary.

(2) The fluffy layer shows the growth of the integral activity of the microorganisms ($^{14}CO_2$– assimilation) as compared to the suprabottom water and surface sediment.

(3) The maximal values of the total number of microorganisms (up to 17.5×10^6 cells mL^{-1}) are observed in the fluffy layer.

(4) The water–sediment boundary zone (the fluffy layer) is provided by the particulate organic matter, which promotes the activity of the heterotrophs from the overlying water column, and by reduced compounds ($N\text{-}NH_4$, HS^-, CH_4^-, Fe^{2+}, Mn^{2+}, and others), which are required for the activity of the autotrophic microorganisms from the underlying sediments.

(5) The presence of active autotrophs (thionic and nitrifiers) in the fluffy layer is confirmed by the growth of the CO_2 assimilation in experiments with the addition of sodium thiosulfate and ammonium nitrogen.

(6) The fluffy layer shows a decrease in the oxygen content and the growth of the dissolved biogenic elements and sulfate ion as compared to the water column; the increase in the sulfate ion is caused by the oxidation of reduced sulfur supplied from the sediments.

(7) An increase in the number of microorganisms in the fluffy layer is accompanied by an increase in the C_{14}–C_{20} n-alkanes.

(8) The maximal biomass of the microorganisms is usually observed in the fluffy layer, where its isotopically heavy (from −18 to −20‰) composition results in the enrichment of the isotopic composition of the total C_{org} in the ^{13}C as compared to the C_{org} from the water column and the sediments.

(9) The change in the isotopic composition of the C_{org} in the fluffy layer (and in the sediment) relative to the C_{ogr} in the particulate matter of the water column presumably represents a widely spread phenomena supporting the leading role of microorganisms in the transformation of the particulate matter at the water–sediment boundary in the Arctic shelf seas.

ACKNOWLEDGMENTS

We are grateful to the captain and team of the R/V *Akademik Mstislav Keldysh*, as well as to the researchers from the Institute of Oceanology of the Russian Academy of Sciences, for their participation in the works onboard the ship, which provided obtaining material for this study. The researchers from the Institute of Oceanology of the Russian Academy of Sciences and from the Vinogradskii Institute of Microbiology of the Russian Academy of Sciences are thanked for their participation in the laboratory studies.

The work was carried out with financial support from the Russian Foundation for Basic Research (project nos. 11-05-12009-ofi-m and 12-05-00210-a), Program 23 of the RAS Presidium, and an RF Presidential Grant (no. NSh-618.2012.5).

REFERENCES

1. N. A. Belyaev, V. I. Peresypkin, and M. S. Ponyaev, "The organic carbon in the water, the particulate matter, and the upper layer of the bottom sediments of the West Kara Sea," Oceanology (Engl. Transl.) **50** (5), 706–715 (2010).
2. A. N. Belyaeva, L. A. Madureira, and J. Eglinton, "Geochemistry of lipids in bottom deposits of the Kara Sea," in *General Studies of Geochemistry. To 100th Anniversary of Academician A.P. Vinogradov* (Nauka, Moscow, 1995), pp. 260–274.
3. A. M. Bol'shakov and A. V. Egorov, "The results of gasometric studies in the Kara Sea," Okeanologiya (Moscow, Russ. Fed.) **35** (3), 399–404 (1995).
4. I. I. Volkov and N. N. Zhabina, "Methods for determination of different sulfur compounds in marine deposits," in *Chemical Analysis of Marine Deposits* (Nauka, Moscow, 1980), pp. 5–27.
5. E. M. Galimov, L. A. Kodina, O. V. Stepanets, and G. S. Korobeinik, "Biogeochemistry of the Russian Arctic. Kara Sea: research results under the Sirro project, 1995–2003," Geochem. Int. **44** (11), 1053–1104 (2006).
6. V. F. Gal'chenko, "Sulphatereducing, methane formation, and methane oxidation in different reservoirs of Banger Hills oasis, Antarctic," Mikrobiologiya **63** (4), pp. 683–698 (1994).
7. Z. N. Gorbunova, "Clay-size minerals in the Kara Sea sediments," Okeanologiya (Moscow, Russ. Fed.) **37** (5), 709–712 (1997).
8. A. I. Danyushevskaya, V. I. Petrova, D. S. Yashin, et al., *Organic Matter of Bottom Sediments of the Polar Zones of the World Ocean* (Nedra, Moscow, 1990) [in Russian].
9. M. V. Ivanov, A. Yu. Lein, E. E. Zakharova, and A. S. Savvichev, "Carbon isotopic composition in suspended organic matter and bottom sediments of the East Arctic seas," Microbiology **81** (5), 596–605 (2012).
10. M. V. Ivanov, A. S. Savvichev, and A. Y. Lein, "Effect of phytoplankton and microorganisms on the isotopic composition of organic carbon in the Russian Arctic seas," Microbiology **79** (5), 567–582 (2010).
11. M. D. Kravchishina, *Suspended Matter of the White Sea and Its Granulometric Composition* (Nauchnyi Mir, Moscow, 2009) [in Russian].
12. M. A. Levitan, Yu. A. Lavrushin, and R. Stein, *The History of Sedimentation in the Arctic Ocean and the Subarctic Seas during Last 130 Thousand Years* (GEOS, Moscow, 2007) [in Russian].
13. A. Y. Lein, N. A. Belyaev, M. D. Kravchishina, et al., "Isotopic markers of organic matter transformation at the water-sediment geochemical boundary," Dokl. Earth Sci. **436** (1), 83–87 (2011).
14. A. Y. Lein, M. D. Kravchishina, N. V. Politova, N. V. Ul'yanova, V. P. Shevchenko, A. S. Savvichev, E. F. Veslopolova, I. N. Mitskevich, M. V. Ivanov, et al., "Transformation of particulate organic matter at the water-bottom boundary in the Russian Arctic Seas: evidence from isotope and radioisotope data," Lithol. Mineral. Resour. **47** (2), 99–128 (2012).
15. A. Y. Lein, Yu. M. Miller, B. B. Namsaraev, et al., "Biogeochemical processes in the sulfur cycle at early stages of diagenesis of sediments in the junction region of Yenisei River and Kara Sea," Okeanologiya (Moscow, Russ. Fed.) **34** (5), 681-692 (1994).
16. A. Yu. Lein, I. I. Rusanov, A. S. Savvichev, et al., "Biogeochemical processes of the sulfur and carbon cycles in the Kara Sea," Geochem. Int. **34** (11), 925–941 (1996).
17. A. P. Lisitsyn, *Oceanic Sedimentation. Lithology and Geochemistry* (Nauka, Moscow, 1978) [in Russian].
18. P. N. Makkaveev, P. A. Stunzhas, Z. G. Mel'nikova, P. V. Khlebopashev, and S. K. Yakubov, "Hydrochemical characteristics of the waters in the western part of the Kara Sea," Oceanology (Engl. Transl.) **50** (5), 688–697 (2010).
19. I. N. Mitskevich and B. B. Namsaraev, "Population size and distribution of bacterioplankton in the Kara Sea in the September of 1993," Okeanologiya (Moscow, Russ. Fed.) **34** (5), 704–708 (1994).
20. B. B. Namsaraev, I. I. Rusanov, I. N. Mitskevich, et al., "Bacterial oxidation of methane in estuary of Yenisei River and Kara Sea," Okeanologiya (Moscow, Russ. Fed.) **35** (1), 88–93 (1995).
21. V. I. Peresypkin and E. A. Romankevich, *Biogeochemistry of Lignin* (GEOS, Moscow, 2010) [in Russian].

22. A. G. Rozanov and I. I. Volkov, "Bottom sediments of Kandalaksha Bay in the White Sea: the phenomenon of Mn," Geochem. Int. **47** (10), 1067–1085 (2009).

23. A. G. Rozanov, V. A. Chechko, and N. M. Kokryatskaya, "Redox profile of bottom sediments in estuary of Ob River," Okeanologiya (Moscow, Russ. Fed.) **35** (1), 850–861 (1995).

24. E. A. Romankevich and A. A. Vetrov, *Carbon Cycle in Arctic Seas of Russia* (Nauka, Moscow, 2001) [in Russian].

25. E. A. Romankevich, A. I. Danyushevskaya, A. N. Belyaeva, and V. P. Rusanov, *Biogeochemistry of Organic Matter in the Arctic Sea* (Nauka, Moscow, 1982) [in Russian].

26. A. S. Savvichev, E. E. Zakharova, E. F. Veslopolova, et al., "Microbial processes of the carbon and sulfur cycles in the Kara Sea," Oceanology (Engl. Transl.) **50** (6), 893–908 (2010).

27. O. V. Shishkina, *Geochemistry of Marine and Oceanic Pore Waters* (Nauka, Moscow, 1972) [in Russian].

28. Boudreau B., *Diagenetic models and their implementation: modeling transport and reactions in aquatic sediments* (Springer, Berlin, 1997).

29. B. O. Ekpo, O. E. Oyo-Ita, and H. Wehner, "Even n-alkane/alkene predominances in surface sediments from the Calabar River, SE Niger Delta, Nigeria," Naturwissenshaften **92**, 341–346 (2005).

30. V. O. Elias, B. R. T. Simoneit, and J. R. Cardoso, "Even n-alkane predominances on the Amazon shelf and a northeast Pacific hydrothermal system," Naturwissenshaften **84**, 415–420 (1997).

31. K. Fahl, R. Stein, B. Gaye-Haake, et al., "Biomarkers in surface sediments from the Ob and Yenisei estuaries and the southern Kara Sea: evidence for particulate organic carbon sources, pathways and degradation," in *Siberian Rivers Run-Off in the Kara Sea*, Ed. by R. Stein, et al. (Elsevier, Amsterdam, 2003), pp. 329–349.

32. I. N. McCave, "Particulate size spectra, behavior, and origin of nepheloid layers over the Nova Scotian Continental Rise," J. Geophys. Res., C: Oceans Atmos. **88** (C12), 7647–7666 (1983).

33. B. Meon and R. M. W. Amon, "Heterotrophic bacterial activity and fluxes of dissolved free amino acids and glucose in the Arctic rivers Ob, Yenisey and the adjacent Kara Sea," Aquat. Microbiol. Ecol. **37**, 121–135 (2004).

34. C. Muller and R. Stein, "Grain-size distribution and clay-mineral composition in surface sediments and suspended matter of the Ob and Yenisei rivers," Ber. Polarforsch **300**, 179–187 (1999).

35. R. J. Nachman, "Unusual predominance of even carbon hydrocarbons in an Antarctic food chain," Lipids **20** (9), 629–633 (1985).

36. S. B. Reinhardt and E. S. van Vleet, "Hydrocarbons of Antarctic midwater organisms," Polar Biol. **6**, 47–51 (1986).

37. H. D. Schulz, "Quantification of early diagenesis: dissolved constituents in marine pore waters," in *Marine Geochemistry* (Springer, Berlin, 2000), pp. 87–128.

38. V. P. Shevchenko, A. P. Lisitzin, V. M. Kuptsov, et al., "The composition of aerosols over the Laptev Sea, the Kara, Barents, Greenland, and Norwegian Seas," in *Russian-German Cooperation: Laptev Sea System* (Alfred-Wegener Institut für Polar- und Meeresforschung, Bremen, 1995), pp. 7–16.

39. R. Stein, *Arctic Ocean Sediments Processes, Proxies and Paleoenvironment* (Springer, Amsterdam, 2008).

40. *The Global Biogeochemical Sulfur Cycle*, Ed. by M. V. Ivanov and J. R. Freney (Wiley, Chichester, 1983).

Translated by M. Bogina